

1 **In-situ unsaturated zone stable water isotope ( $^2\text{H}$  and  $^{18}\text{O}$ )**  
2 **measurements in semi-arid environments using tunable**  
3 **off-axis integrated cavity output spectroscopy.**

4

5 **M. Gaj<sup>1,2</sup> M. Beyer<sup>1</sup>, P. Koeniger<sup>1</sup>, H. Wanke<sup>3</sup>, J. Hamutoko<sup>3</sup>, T. Himmelsbach<sup>1</sup>**

6 [1]{Federal Institute for Geosciences and Natural Resources (BGR), Stilleweg 2, Hannover,  
7 Germany}

8 [2]{Chair of Hydrology, Faculty of Environment and Natural Resources, University of  
9 Freiburg, Fahrenbergplatz, 79098 Freiburg, Germany}

10 [3]{University of Namibia, (UNAM) Windhoek, Namibia}

11

12 Correspondence to: Marcel Gaj (marcel.gaj@bgr.de)

13

14

1 **Abstract**

2 Stable isotopes (deuterium,  $^2\text{H}$ , and oxygen-18,  $^{18}\text{O}$ ) of soil pore water were measured directly  
3 in the field using tunable off-axis integrated cavity output spectroscopy (OA-ICOS) and  
4 commercially available soil gas probes in a semi-arid region of the Cuvelai-Etosha-Basin,  
5 Namibia. High spatial and temporal resolution was achieved in the study area with reasonable  
6 accuracy and measurements were in agreement with laboratory-based cryogenic vacuum  
7 extraction and subsequent cavity ring down laser spectroscopic isotope analysis (CRDS).  
8 After drift correction of the isotope data, precision for over 140 measurements of two  
9 consecutive field campaigns in June and November, 2014 were 1.8 ‰ and 0.48 ‰ for  $\delta^2\text{H}$   
10 and  $\delta^{18}\text{O}$ , respectively. Mean accuracy using quality check standards was -5 ‰ and 0.3 ‰ for  
11  $\delta^2\text{H}$  and  $\delta^{18}\text{O}$ , respectively. Results support the applicability of an in-situ measurement system  
12 for the determination of stable isotopes in soil pore water. Spatio-temporal variability could  
13 be deduced with the observed data in an extremely dry evaporation dominated environment  
14 which was sporadically affected by intermittent rainfall. Finally, water isotope depth profiles  
15 are used quantitatively to calculate a soil water balance

16

17

## 1 **1 Introduction**

2 The advantage of hydrogen and oxygen stable isotopes in water (e.g. deuterium,  $^2\text{H}$  and  
3 oxygen-18,  $^{18}\text{O}$ ) compared to other tracers is the areal input. Precipitation shows a linear  
4 relationship between water  $^2\text{H}$  and  $^{18}\text{O}$  isotopic composition on a global scale. This  
5 relationship is known as the global meteoric water line (GMWL) (Craig, 1961). Meteoric  
6 water tends to be more depleted in  $^2\text{H}$  and  $^{18}\text{O}$  in higher latitudes. This can also be observed  
7 when they are moving further inwards a continent (Dansgaard, 1964). Therefore, rainfall  
8 isotope data at particular locations can plot on a local meteoric water line (LMWL) with a  
9 different slope than the GMWL.

10 The isotopic composition of precipitation in any region is, driven primarily by local altitude  
11 and seasonal climatic patterns, while single event variation is caused by the type of event. For  
12 example, short and heavy rainfall events (e.g., convective) tend to be more enriched than  
13 those with longer duration. This is known as the amount effect and leads to distinguishable  
14 isotopic composition of single events (Clark and Fritz, 1997). Hence, the stable isotope  
15 composition of precipitation reveals information of single and local events as well as of  
16 seasonal and continental circulation patterns. However this input signal is altered during  
17 infiltration through evaporation, dispersion and mixing of water with different isotopic  
18 composition. Evaporation leads to enrichment in the remaining reservoir and changes in  
19 deuterium excess values. Heterogeneous flow paths and variable storage capacities in  
20 different subsurface reservoirs contain old water with potentially different isotopic  
21 composition as the new input. Soil types, and different landscape positions characterize  
22 evaporation patterns and therewith enrichment of water on its way through and into the  
23 unsaturated zone.

24 Further, stable isotopes have been successfully used for decades as powerful proxies for the  
25 description of water fluxes such as infiltration in humid (Saxena, 1987) or semi arid regions  
26 (Dincer et al., 1974; Allison and Hughes, 1983), evapotranspiration (Barnes and Allison,  
27 1988, Skrzypek et al., 2015), plant root water uptake (Dawson and Ehleringer, 1991;  
28 Ehleringer and Dawson, 1992; Dawson, 1996; Yang et al., 2010), hydraulic redistribution  
29 (Dawson, 1993; Caldwell et al., 1998), and in catchment hydrology (e.g., Sklash and  
30 Farvolden, 1979; Richard and Shoemaker, 1986; Tetzlaff et al., 2007; Kendall and  
31 McDonnell, 2012). Water stable isotopes provide information on flow paths way and mixing  
32 within the unsaturated zone (Gazis and Feng, 2004; Stumpp and Maloszewski, 2010;

1 Garvelmann et al., 2012; Mueller et al., 2014). Soil water stable isotope studies were also  
2 used to reduce parameter uncertainty in unsaturated zone model approaches (Sprenger et al.,  
3 2014).

4 Isotope profiles in the unsaturated zone of arid and semi-arid regions are dominated by  
5 evaporation effects overprinting the input signal of precipitation. Soil evaporation can be  
6 separated into direct evaporation from a water saturated surface (stage I) and diffusion  
7 controlled vapor transport (stage II) (Or et al., 2013). At the evaporating front the dominance  
8 of one of the two processes changes. The depth can be theoretically determined and is  
9 characterized by the strongest isotope enrichment. Actual evaporation rates can be  
10 determined using isotope depth profiles by applying analytical solutions, for stationary  
11 isothermal and non-isothermal cases developed by Barnes and Allison, (1983). Evaporation  
12 from water stored in the unsaturated zone initially plotted on the LMWL tends to fall on a  
13 specific evaporation line with a slope dependent on atmospheric temperature and relative  
14 humidity as well as the substrate (Allison et al., 1983; Barnes and Allison, 1988). The  
15 intersection of that evaporation line with the LMWL is known to be the mean isotopic  
16 composition of the originating water.

17 Intensive work has been done to use stable isotopes for quantitative recharge estimations and  
18 is actively discussed in early and recent reviews (e.g., Allison et al., 1994; Scanlon et al.,  
19 2002). But the usefulness of evaporation profiles to determine recharge remains debatable  
20 (Herczeg et al, 2011).

21 In all unsaturated zone studies manual removal of soil samples and a subsequent extraction of  
22 soil water in the laboratory was necessary using either vacuum extraction (e.g., West et al.,  
23 2006; Koeniger et al., 2011; Orłowski et al., 2013), equilibration (e.g., Wassenaar et al.,  
24 2008), mechanical squeezing, azeotropic distillation or centrifugation methods (e.g., Walker et  
25 al., 1994; Kelln et al., 2001). These methods cause both disturbance to the integrity of the  
26 natural soil system and possible evaporation during the sampling procedure. The latter is  
27 especially important for dry soils. Hence, soil water extraction techniques are labor intensive  
28 and expensive which is limiting the use of stable isotopes compared to the other state  
29 variables such as soil moisture or matrix potential. Indeed, there are suction cup installations  
30 which allow a removal of soil water non-destructively but are not applicable in arid  
31 environments.

1 However, recent developments in laser spectroscopy allow the measurement of stable isotopes  
2 with much higher throughput and even continuously (Berman et. al., 2009; Herbstritt et al.,  
3 2012). Such measurements are desirable while facing questions concerning eco-hydrological  
4 interactions within the soil plant atmosphere which are not yet fully understood (McDonnell,  
5 2014). In atmospheric studies their sensitivity to vapor concentrations as well as their long-  
6 term behavior was already addressed (Wang et al., 2009; Schmidt et al., 2010; Sturm and  
7 Knohl, 2010; Johnson et al., 2011; Rambo et al., 2011; Aemisegger et al., 2012). Since new  
8 laser spectrometers are available, continuous measurements of the isotopic composition from  
9 transpired water is possible (Wang et al., 2012) and when combined with isotope depth  
10 profiles also a separation of evapotranspiration can be obtained (Dubbert, 2013). By now,  
11 using hydrophobic gas permeable membranes enables the measurement of stable isotopes in  
12 liquid water with a temporal resolution of less than a minute (Herbstritt et al., 2012).

13 Principles to sample soil air for the determination of stable isotopes were already indicated by  
14 Allison et al., (1987) and Schack-Kirchner et al., (1993). An attempt to measure stable  
15 isotopes in a sandy loam using a liquid water analyzer (OA-ICOS, Los Gatos Research, DLT-  
16 100) is presented in a recent review by Soderberg et al., (2012). The first study monitoring  
17 stable isotopes in-situ in unsaturated sandy soil water under laboratory conditions made use of  
18 poly-propylene (PP) membranes (Rothfuss et al., 2013). Measurements were performed with  
19 a cavity-ring-down spectrometer (CRDS) (L1102-I, Picarro, CA, USA) calibrated with liquid  
20 water injections using a vaporizer unit. Volkmann and Weiler, (2014) developed custom built  
21 poly-ethylene (PE) probes with an equilibration chamber allowing additional mixing of the  
22 vapor to prevent condensation in the sample line. They further proposed a sophisticated  
23 system with a CRDS device (Picarro L2120-i, CA, USA) calibrated with standards prepared  
24 on prior oven dried local substrate.

25 In the present study in-situ usability of commercially available PP–membranes (BGL-30,  
26 Umweltmesssysteme, Munich) using a liquid water analyzer (Los Gatos Research, DLT-100)  
27 for a determination of stable isotopes in soil pore water is demonstrated. In comparison to  
28 earlier in-situ studies this study presents an improved automatization and minimal technical  
29 effort. The in-situ measurements are compared to data derived through cryogenic vacuum  
30 extraction in the laboratory in order to verify the in-situ applicability. Besides, the proposed  
31 system is for the first time applied under semi-arid and remote field conditions on dry sandy  
32 soils with moisture contents ranging from 0.3 to 6 %. Infiltration and evaporation patterns as

1 well as effects caused by strong temperature changes are discussed. The present study shows  
2 for the first time an application of in-situ measurements of water stable isotopes in the  
3 unsaturated zone under field conditions. **The main hypotheses are:**

- 4 - **Commercially available soil gas probes are applicable for measurement of water stable**  
5 **isotopes in soil pore water.**
- 6 - **The system is applicable in a semi-arid environment for water contents lower than 5%**
- 7 - **Results derived from destructive sampling and a subsequent soil water extraction**  
8 **using a cryogenic-vacuum extraction, equal those from in-situ measurements**

9  
10 **In addition, the derived isotope data is used quantitatively to determine a soil water balance of**  
11 **a thick sandy unsaturated zone.** Further unique is the mode of automatisation, utilizing the  
12 interface of the common laboratory autosampler, which allows a laboratory like operation.  
13 The potential limitations of in-situ systems under dry conditions with high temperature and  
14 humidity gradients are discussed.

## 15 **2 Study Site and Methods**

16 The study area is located in the north of Namibia and is part of the Cuvelai-Etосha-Basin  
17 (CEB). The whole surface water catchment has an extent of about 173,000 km<sup>2</sup> where the  
18 northern part (approx. 52,000 km<sup>2</sup>) belongs to Angola and the southern part to Namibia. This  
19 sedimentary basin is divided into four major sub-basins called Iishana, Niipele, Olushandja  
20 and Tsumeb and can be further separated into different drainage zones. Measurements were  
21 conducted within the eastern sand zone close to the township of Elundu as indicated in Figure  
22 1.

23 The assignment of the catchment and its sub-basins is based on geography, population  
24 distribution and water infrastructure (Dragnich et al., 2004). The main shallow aquifer system  
25 in the CEB is a multilayer aquifer system in the Andoni formation with a thickness of 6 to 80  
26 m. The main groundwater flow is towards the Etosha pan with an average gradient of 0.2 %  
27 (Christelis and Struckmeier, 2001). Beside the shallow aquifer, recent studies identified an  
28 area of 500 km<sup>2</sup> potentially containing fresh groundwater at a depth of 200 m namely the  
29 Ohangwena II aquifer (Lindenmaier and Christelis, 2012; Lindenmaier et al., 2014).  
30 Groundwater recharge mechanisms concerning both, the shallow and the deep aquifer are not  
31 yet fully understood. The shallow aquifer system consists partly of freshwater lenses on  
32 brackish to saline groundwater mostly in the Iishana region. Perched discontinuous aquifers

1 are found in the eastern part of the basin and can develop on clay lenses in the subsurface  
2 managed through hand-dug wells.

3 The climate in the CEB is semi-arid with a rainy season lasting from November to April and a  
4 dry season from May to October. Annual average potential evaporation can reach up to 3,000  
5 mm and decreases slightly from north to south (Mendelsohn et al., 2013). Annual average  
6 rainfall ranges between 250 and 600 mm with most of the rain is falling in January and  
7 February (Mendelsohn et al., 2013). The eastern part of the catchment receives more  
8 consistent rainfall whereas the rainfall in the western part is less predictable.

9 The investigated site is forested, predominantly vegetated with *Combretum collinum*, *Acacia*  
10 *erioloba* and *Baikiea plurijuga*. The deep Kalahari sand can reach a depth of over 40 meters  
11 and has high saturated hydraulic conductivity ( $2304\text{cm day}^{-1}$  –  $2409\text{cm day}^{-1}$ ) determined  
12 with double-ring infiltration experiments, high porosity (0.4) and low field capacity (~ 3.5%).  
13 Sampling and measurements were conducted during two field campaigns. The first field  
14 campaign was conducted between the 9<sup>th</sup> and 15<sup>th</sup> of June 2014 and the second between 15<sup>th</sup>  
15 and 22<sup>th</sup> of November 2014. To determine heterogeneity of infiltration and evaporation  
16 processes and to evaluate an in-situ approach determining stable isotopes in soil water nine  
17 plots within an area of 9,000m<sup>2</sup> were investigated. During the first campaign soil gas probes  
18 were installed at depths of 2 cm, 5 cm, 10 cm, 15 cm, 20 cm, 25 cm, 30 cm, 40 cm and 50 cm.  
19 Two plots were established with different vegetation characteristics such that one was  
20 vegetated with shrubs and the other was exposed without any vegetation. During the second  
21 field campaign probes were installed at depths of 2 cm, 5 cm, 7.5 cm, 10 cm, 12.5 cm, 15 cm  
22 17.5 cm 20 cm, 25 cm, 30 cm, 40 cm, 50 cm, 60 cm, 70 cm, 80 cm, 90 cm, and 100 cm to  
23 reach a maximum resolution especially for the top layer. In addition to the in-situ  
24 measurements samples were collected in head space glass vials for laboratory extraction and  
25 crimp sealed to avoid evaporation. Soil moisture measurements were conducted with a time  
26 domain reflectometry system (TDR, EasyTest, Poland) at the beginning of each  
27 measurements cycle with the same resolution. Samples were transported via aircraft to the  
28 laboratory of the Federal Institute of Geosciences and Natural Resources (BGR) in Hannover,  
29 Germany and subsequently extracted.

30 In the laboratory grain size analyses was conducted on 10 g material from the extracted  
31 samples < 2000  $\mu\text{m}$  was washed and particles < 63  $\mu\text{m}$  were allowed to pass a < 63  $\mu\text{m}$  sieve.  
32 The sand fraction (63-2000  $\mu\text{m}$ ) was dried again and the amount of material < 63  $\mu\text{m}$  was

1 calculated by difference between initial and recovered sample mass. The grain size analysis of  
2 the dried sand was performed using an optically based instrument (Camsizer, Retsch). The  
3 instrument employs two digital cameras (CCD) to record falling particles (dynamic image  
4 analysis) in the grain size of 0.03-30.0 mm. The instrument images a falling curtain of  
5 sediment and determines the grain size of each particle in the image using two different  
6 cameras. Typically images of a few million grains were processed for each sample (Altuhafi  
7 et al., 2013).

8 For stable isotope analysis of soil water triplicate soil samples were prepared and scaled  
9 before and after the water extraction procedure. **The standard deviation determined from each**  
10 **triplet is used as an additional analytical error.** Soil water was extracted cryogenically using a  
11 slightly modified method of the cryogenic-vacuum extraction described by Koeniger et al.,  
12 (2011). Instead of a water bath heated by a hot plate an isolated aluminium block tempered  
13 to 105 °C was used. Each sample was evacuated at -3mbar vacuum and extracted for 15 min  
14 after shock freezing. Subsequent, soil samples were oven dried at 105°C for 24h and weighted  
15 again. Results before and after oven drying are compared as a measure of extraction success.  
16 The water samples were subsequently measured with a cavity ring-down spectrometer  
17 (CRDS, model L2120-i, manufactured by Picarro Inc.). <sup>18</sup>O/<sup>16</sup>O and <sup>2</sup>H/<sup>1</sup>H isotope ratios are  
18 normalized on the international δ- scale and expressed as parts per thousand:

$$19 \quad \delta = \left[ \left( \frac{R_{sample}}{R_{reference}} \right) - 1 \right] \text{‰} \quad [1]$$

20 where R<sub>sample</sub> (-) denotes the <sup>18</sup>O/<sup>16</sup>O isotope ratio (respectively <sup>2</sup>H/<sup>1</sup>H) of a water sample and  
21 R<sub>standard</sub> (-) those of the Vienna Standard Mean Ocean Water (VSMOW). All values were  
22 corrected for drift and memory applying a method proposed by van Geldern and Barth (2012).  
23 Accuracies for long-term quality check standards are better than 0.2 ‰ and 0.8 ‰ for water  
24 samples, but an additional error for sandy soil extractions has to be taken into account which  
25 is better than 0.8 and 4 ‰ for δ<sup>18</sup>O and δ<sup>2</sup>H, respectively (Königer et al., 2011). Subscripts are  
26 used to distinguish between either the in-situ (I) and the cryogenically (C) derived isotope  
27 values in the remaining text.

28 For the determination of δ<sup>2</sup>H<sub>I</sub> and δ<sup>18</sup>O<sub>I</sub>, commercially available soil gas probes (BGL-30,  
29 Umweltmesssysteme, Munich (UMS)) with a diameter of 9.4 mm and a length of 300 mm  
30 were connected to an integrated cavity off-axis liquid water isotope analyser (OA-ICOS, Los  
31 Gatos research, DLT100). **This device does not measure continuously and maintenance of the**



1 communication via the laboratory autosampler interface is mandatory. A simplified wiring  
2 diagram is illustrated in figure 2. Each probe is separated from the main transport line with a  
3 valve (Clippard Minimatic, USA) which in turn is controlled by the control lines data terminal  
4 ready (DTR) and request to send (RTS) of a modified USB-to-RS232 converter connected to  
5 a laptop computer. To secure the converter by inverse currents a common diode is set in  
6 inverse direction to the optocoupler (ULN2303). A reduction of the electric tension output of  
7 the converter is necessary using a resistor with 220  $\Omega$ . Finally, the laptop computer is  
8 communicating with the OA-ICOS through the same RS-232 connection. The laptop  
9 computer mimics the behavior of a laboratory autosampler via a python script. To avoid over  
10 heating of the analyser during day time by direct sun radiation a gazebo was positioned above  
11 the loading area of the pick-up truck where the analyser is mounted. Power supply was  
12 maintained using a common 230 V generator.

13 Four repetitive measurements at each depth were performed during the first campaign. During  
14 the second campaign six consecutive measurements were performed at each depth. A  
15 measurement cycle consists of three steps: i.) a flushing phase where the cavity is evacuated,  
16 ii.) the sample intake opening a particular valve and iii.) the measurement of the sample.  
17 Flushing introduces a vacuum of 0.1torr or less. The sample intake is controlled by valves  
18 which are opened for 10 s for each measurement allowing a volumetric flow between 95 and  
19 110 ml/min. The transported gas volume is measured with a flow control device (Analyt-  
20 MTC 0-200 ml min<sup>-1</sup>). The probe and transport lines to the analyser have a volume of  
21 approximately 40 ml. The lines are made of steel and are connected with Swagelok<sup>®</sup>  
22 connectors. After six consecutive measurements at one depth, the sampled soil volume is  
23 approximately 120 ml. Assuming that the soil volume around the 300 mm long probe is  
24 sampled equally over the whole length, a diameter of 1cm around the probe will be directly  
25 affected by the uptake of vapour via the probe. Hence the top layer is measured with  
26 reasonable accuracy for this particular setup. The measurement of a 1m deep profile  
27 considering 16 different depths with 6 repetitions and a resolution down to 2.5 cm for the top  
28 20 cm takes about 4.5 hours. The OA-ICOS device needs an additional warm up of about two  
29 hours.

30 Standard preparation of 200g prior oven dried sandy substrate was used. It has been  
31 transported in aluminium bags (WEBA bags ©) and was spiked with 5 ml of standard before  
32 the experiment at the day of measurement. Normalization to the international scale is done

1 using one low standard (HGLA) and one high standard (HMER). In addition one standard for  
 2 drift correction (HDES) and a quality check standard (HLAU) were used. The quality check  
 3 standard is treated as an unknown sample. All standards were measured at the beginning of  
 4 each experimental sequence; additionally HDES and HLAU were measured at the end of each  
 5 sequence. Isotope values of the used standards are illustrated in table 1. The standards were  
 6 used only for two consecutive measurement series and then new standards were prepared to  
 7 avoid potential enrichment through evaporation. Calibration standards were kept in flasks  
 8 with a diameter of 2 cm and a length of 50 cm. Soil gas probes were subsequently entered and  
 9 the flasks sealed to avoid evaporation.

## 10 **Soil water balance**

11 Recharge rates are determined using a simple empirical relationship applied to the data of the  
 12 deep isotope depth profiles. The relationship for  $\delta^2\text{H}$  is given as (Clark and Fritz, 1997):

$$13 \quad R = \left[ \frac{22}{\delta^2\text{H}_{shift}} \right] \quad [2]$$

14 and for  $\delta^{18}\text{O}$  as

$$15 \quad R = \left[ \frac{3}{\delta^{18}\text{O}_{shift}} \right] \quad [3]$$

16 A linear regression is applied to the deep isotope depth profile and the shift to the LMWL is  
 17 determined (Figure 4). Soil Evaporation is calculated from the isotope depth profiles using an  
 18 analytical solution (Allison et al., 1984).

$$19 \quad E = (1 - h_a) N_{sat} \tau D^v \frac{(p - \theta_v)}{\rho z_{ef}} \quad [4]$$

20 Though, evaporation can be determined providing the relative humidity  $h_a$ , the saturated  
 21 water vapor pressure, the tortuosity with  $\tau=0.66$ , the diffusivity of water vapor in air  
 22  $D^v = 24 * 10^{-4}$ , the density of water  $\rho$ , the porosity  $p$  and the soil water content  $\theta_v$ . The  
 23 depth of the evaporation front  $z_{ef}$  can be determined by an exponential fit to the isotope depth  
 24 profiles (Allison et al., 1985).

$$25 \quad \delta = \delta_{res} (\delta_{ef} - \delta_{res}) \exp^{-z/z_{ef}} \quad [5]$$

1 The isotope ratio  $\delta$  at depth  $z_{ef}$  is then calculated from the isotope value of the reservoir  $\delta_{res}$   
2 and the isotope ratio at the evaporating front  $\delta_{ef}$ . Calculations were conducted for a mean  
3 ambient temperature of 24°C and 60% relative air humidity. This will give a quantitative  
4 estimation of the soil water balance based on the presented isotope data.

5 In addition  $z_{ef}$  is determined from grain the grain size distribution as follows (Or et al., 2013):

$$6 \quad z_{ef} = \frac{2\alpha}{\rho g \left( \frac{1}{r^1} - \frac{1}{r^2} \right)} \quad [5]$$

7 with the surface tension of water  $\alpha$  at 24°C, the minimum  $r^1$  and the maximum  $r^2$  grain size of  
8 the soil.

### 9 **3 Results**

#### 10 **Campaign 1**

11 The first field campaign was conducted short after the rainy season. No rain occurred during  
12 that campaign. The texture (medium sand) was uniform throughout the depth profile. No  
13 changes in texture were observed for the other investigated plots. Temperature and humidity  
14 variability within the sampling period between daytime ( $\sim 30^\circ\text{C}_{\text{max}}$  and  $15\%_{\text{min}}$ ) and night ( $\sim$   
15  $9^\circ\text{C}_{\text{min}}$  and  $\sim 90\%_{\text{max}}$ ) was high during the first campaign.

16 During the first campaign (15<sup>th</sup> of June 2014) measurements were taken at two plots (E1.1,  
17 E1.2) at a distance of 25 meters on the same day. The measurement at E1.1 started at 09:30  
18 and later at 16:00 at plot E1.2. Plot E1.1 is not vegetated and has a thin soil crust in the top  
19 first centimeter. Volumetric water content increases from 0.3 % at the top to 4.1% at 50 cm  
20 depth (Figure 3, left). Plot E1.2 is vegetated, a dense root mat is visible in the upper 10 cm. In  
21 contrast to E1.1 water contents are much lower increasing from 0.3 % at the surface to 0.7 %  
22 at 50 cm depth (Figure 3, center). The isotope depth profiles are of similar shape and  
23 magnitude for both profiles with a maximum at 10 cm and an exponential decline down to the  
24 maximum depth. Due to low water contents in the upper 15 cm of the vegetated plot, not  
25 enough water could be extracted with the cryogenic extraction method. However, at 10 cm  
26 depth the same pattern as for profile E1.1 can be observed. The shape of the isotope depth  
27 profiles is different for  $\delta^{18}\text{O}$  and  $\delta^2\text{H}$  within the upper 5 to 10 cm. As depicted in Figure 5, the  
28 deuterium excess for both profiles shows a maximum at 10 cm depth and are exponentially  
29 decline down to 50cm. At the vegetated plot deuterium excess values are positive within the  
30 top 7.5cm. Comparing deuterium excess values of the cryogenic extraction with those from

1 the in-situ measurements it can be found that they agree well for the bare soil plot, but not at  
2 10cm and 15cm depth. In contrast, all values measured in the field below 10cm of the  
3 vegetated plot, which has very low water contents (< 1%), are shifted towards more positive  
4 values.

## 5 **Campaign 2**

6 During the second campaign variations in temperature and humidity were much smaller  
7 compared to Campaign 1 (daytime ~35 °C<sub>max</sub> and 30 %<sub>min</sub>; night ~20 °C<sub>min</sub> and ~ 90 %<sub>max</sub>).  
8 Two rainfall events were recorded (12<sup>th</sup> of November 2014: 12 mm morning, 13<sup>th</sup> of  
9 November 2014 30 mm morning) at the climate station in Eenhana which is approximately 15  
10 kilometers west of the experimental site. However, there is no isotope data available until the  
11 17<sup>th</sup> of November. Later during the campaign small rain events (16mm) could be sampled for  
12 isotopes on the 17<sup>th</sup> of November 2014 at 8:00 a.m. with -0.6 ‰ and 3.0 ‰ for  $\delta^{18}\text{O}$  and  $\delta^2\text{H}$ ,  
13 respectively. Another event (4mm) was sampled at the 19<sup>th</sup> of November 2014 with isotope  
14 values of 3.6 ‰ and 28.8 ‰ for  $\delta^{18}\text{O}$  and  $\delta^2\text{H}$ .

15 In contrast to the plots measured during the first campaign, the plots in November (rainy  
16 season) show higher water contents and variable vegetation patterns. One unvegetated plot of  
17 the second campaign (E2.7, see Fig. 4 right hand side and Table 2) is used to compare the in-  
18 situ and the laboratory results as an example with higher water contents. The water contents  
19 range between 4.4 % and 6.8 % with maximum values between 12.5 cm and 25 cm (Figure 3,  
20 right). Strongest enrichment of  $\delta^{18}\text{O}$  is in the top layer declining exponentially with depth for  
21 both methods. There is good agreement between  $\delta^{18}\text{O}_I$  and  $\delta^{18}\text{O}_C$  except for the depth at 30  
22 cm and 50 cm. In contrast, there are substantial differences between  $\delta^2\text{H}_I$  and  $\delta^2\text{H}_C$ . Above 25  
23 cm values of  $\delta^2\text{H}_C$  are more enriched (-15.5 to -22.6 ‰) than for  $\delta^2\text{H}_I$  (-25.0 to -29.2‰), and  
24 vice versa depleted below 25 cm with -23.4 to -15.2 ‰ for  $\delta^2\text{H}_C$  and -11.6 to -5.1‰ for  $\delta^2\text{H}_I$   
25 ,respectively.

26 Both isotope depth profiles of the first campaign show good agreement between 15 cm and 50  
27 cm ( $\delta^{18}\text{O}$  RMSE = 3.9;  $\delta^2\text{H}$  RMSE= 9.2) but diverge at shallower depth with more enriched  
28 values for the in-situ measurements ( $\delta^{18}\text{O}$  RMSE = 7.0;  $\delta^2\text{H}$  RMSE= 43.4). In general, better  
29 agreement can be observed for  $\delta^{18}\text{O}$  compared to  $\delta^2\text{H}$  values. Both isotope profiles of the first  
30 campaign derived from the cryogenic vacuum extraction show a maximum at 15 cm with an  
31 exponential decline down to depth. Values of the in-situ measurement show this maximum at  
32 10cm, but only for  $\delta^{18}\text{O}_I$ . The profile of the second campaign does show good agreement

1 within the top 25 cm for  $\delta^{18}\text{O}_I$  but for  $\delta^2\text{H}$  only within the upper 10 cm. In terms of accuracy  
2 for the set of these three profiles we obtain 6.86 ‰ and 1.87 ‰ for  $\delta^2\text{H}_I$  and  $\delta^{18}\text{O}_I$ ,  
3 respectively.

4 A compilation of the quality check standards of the presented campaigns is shown in table 2.  
5 The standard deviation of the repetitive measurements for each depth is a measure of  
6 measurement precision. After drift correction and normalisation of the isotope depth profile  
7 E1.1 the precision ( $\sigma_{qc}$ ) of the quality check standard (HLAU) was 5.2 ‰  $\delta^2\text{H}$  and 0.66 ‰  
8  $\delta^{18}\text{O}$ . The mean precision of the repetitive measurements ( $\sigma_{rep}$ ) is two times better for  $\delta^2\text{H}_I$   
9 than for the precision of the repetitive measurements ( $\sigma_{cry}$ ) for values derived with the  
10 cryogenic vacuum extraction  $\delta^2\text{H}_C$ . Values of  $\delta^{18}\text{O}$  show a higher similarity (refer to table 2).  
11 The measurement of the second profile E1.2 is less precise for  $\delta^2\text{H}_I$  but in the same range as  
12  $\delta^2\text{H}_C$ . Similar precision as for profile E1.1 is found for the third profile E2.7 for both  $\delta^2\text{H}$  and  
13  $\delta^{18}\text{O}$ , respectively.

#### 14 $\delta^{18}\text{O}$ vs $\delta^2\text{H}$

15 In figure 4 the  $\delta^{18}\text{O}$  to  $\delta^2\text{H}$  relationship is shown. The LMWL is derived from historical data  
16 collected in the CEB and has a slope of 7.3 ( $R^2 = 0.96$ ). Additionally, mean values of local  
17 groundwater ( $\sigma^{18}\text{O}=0.91$ ,  $\sigma^2\text{H}=4.27$ ) and soil water down to a depth of 4m with 10cm resolution  
18 are presented. Soil water from the first field campaign derived from the cryogenic vacuum  
19 extraction plots along an evaporation line with a slope of 2.4 ( $R^2 = 0.79$ ) for the non-vegetated  
20 plot and 3.1 ( $R^2= 0.96$ ) for the vegetated plot. In-situ measurements of the non-vegetated plot  
21 have a slope of 3.9 ( $R^2 = 0.84$ ). Excluding the first 10 cm of the unvegetated profile the slope  
22 is 2.9 ( $R^2 = 0.73$ ). Values of the vegetated site derived from the in-situ measurements have a  
23 slope of 3 ( $R=0.464$ ) and are shifted towards more positive  $\delta^2\text{H}$  values. Excluding the top 15  
24 cm of the in-situ measurement the slope remains the same but with  $R^2 = .9$ . Values from the  
25 second campaign show a much higher slope with 5.29 ( $R^2 = 0.75$ ) for the in-situ measurement  
26 and 5.1 ( $R^2 = 0.96$ ) for the cryogenic vacuum extraction and are plotting close to the LMWL.

#### 27 **Spatio-temporal variability**

28 Each profile of the second campaign is measured at 18 different depths and each depth with  
29 six repetitions. After drift correction of the isotope data, the mean precision considering the  
30 quality check measurements ( $\sigma_{qc}$ ) for more than 140 measurement points is 2.15 ‰ for  $\delta^2\text{H}_I$   
31 and 0.36 ‰ for  $\delta^{18}\text{O}_I$  (Table 2). Mean standard deviation of the repetitive measurements ( $\sigma_{rep}$ )  
32 of each depth is 1.86 ‰ for  $\delta^2\text{H}_I$  and 0.46 ‰ for  $\delta^{18}\text{O}_I$ , respectively. As shown in table 2, the

1 mean standard deviation of the repetitive measurements are similar to those derived from the  
2 quality check standards. Differences are observed between  $\sigma_{qc}$  and  $\sigma_{rep}$ . However, the  
3 precision of  $\delta^2H$  is within the range of the mean accuracy of 5.1 ‰. The accuracy of  $\delta^{18}O$  is  
4 much higher with 0.11 ‰. There are two outliers (E2.8, E2.9) which were not considered for  
5 the mean precision or accuracy.

6 Three rows are measured consisting of three plots. Each row is 150m in distance from each  
7 other as well as each profile within one row. Each row is further named as one transect.  
8 Transects consist of bare plots as well as vegetated plots (Table 2). However, lateral roots  
9 could be found at each plot. Mean values of each transect are shown to illustrate an averaged  
10 temporal development with intermittent rainfall (Figure 6) for this particular area. The first  
11 transect is affected only from the first set of rain events (E2.1 to E2.3) and was measured  
12 within two consecutive days. The next transect (E2.4 to E2.6) is affected by the 16 mm event  
13 (17<sup>th</sup> November 2014) of which isotope data is available and the profiles were measured in a  
14 period of three days. Finally, the last three plots (E2.7 to E2.9) had the longest time to recover  
15 from the first rain events and experienced only additional precipitation on the 19<sup>th</sup> Nov 2014  
16 with an amount of 4 mm. Maximum infiltration depth varied between 65 and 95 cm. Water  
17 content varied between 0.5% and 9.5%. Comparing the three transects it can be observed that  
18 variability of isotope depth profiles decreases from the first to the last transect and an  
19 evaporation profile developed.

20 **To account for spatial variability mean values of soil moisture were calculated for each depth**  
21 **of the nine plots. Additionally, the standard deviation of each depth for soil moisture,  $\delta^{18}O$**   
22 **and  $\delta^2H$  are calculated. Figure 7 shows mean soil moisture of each depth against the standard**  
23 **deviation of soil moisture and those of the two isotopes. Basically, high (>4%) and low (<2%)**  
24 **water content has lower variability of soil moisture compared to values between. In contrast,**  
25 **the standard deviation of  $\delta^{18}O$  increases with decreasing soil water content.**

## 26 **Soil water balance**

27 **Recharge estimated from soil water stable isotope data is less than 1% of precipitation. It**  
28 **ranges between 4 – 5 mm derived from  $\delta^2H_{shift}$  and  $\delta^{18}O_{shift}$ , respectively. The evaporation**  
29 **front is determined from the exponential fit to soil water stable isotope depth profiles. Results**  
30 **are summarized in table 3. Annual mean soil evaporation is determined with  $130 \pm 40$  mm/y.**  
31 **The remainder is potentially available for transpiration with  $507 \pm 40$  mm/y. Hence, there is a**  
32 **contribution of  $80 \pm 6$  % of transpiration of total evapotranspiration.**

1 Values of  $z_{ef}$  are between 110 and 290 mm/y which is in agreement with values derived from  
2 a physical model proposed by Or et al., (2013). Considering two different ranges, one for  
3 finer and one for coarser texture, we derive a depth of the evaporation front of 210 and 118  
4 mm for  $r^1 = 63 - 112 \mu\text{m}$  and  $r^2 = 630 - 1120 \mu\text{m}$ , respectively. Calculated soil evaporation  
5 rates for profiles from June 2014 are between 79 - 67 mm/y and 201 - 161 mm/y. The  
6 potential contribution of transpiration / root water uptake at the inter-canopy plot is between  
7 69 and 88 %. At the site underneath the canopy and vegetated with shrubs the contribution is  
8 between 71 and 84 %. This is in agreement with other isotope based studies (Sutanto et al.,  
9 2014). After the rain events during the second field campaign the evapotranspiration pattern is  
10 dominated by soil evaporation. The evaporation front is still developing ( $z_{ef} = 51 - 68 \text{ mm}$ )  
11 and the contribution of transpiration to total evapotranspiration is much lower with 15 - 51%.  
12 Applying this methodology to the different transects, soil evaporation decreases from 4 to  
13 below 1 mm/d.

#### 14 **4 Discussion**

15 The data presented shows potentials, limitations and future research directions that are  
16 required for a deeper understanding of unsaturated zone processes utilizing in-situ methods  
17 for the determination of water stable isotopes. At our particular location we found that  
18 especially the interaction between the top 20 cm of the soil profile and the atmosphere needs  
19 further investigation. Additionally, the transport of water vapor after rain events and its  
20 influence on isotope to depth profiles is not yet fully understood. This is also valid to spatial  
21 variability which can be caused by heterogeneous rainfall even on a small scale, interception  
22 and preferential flow paths that can affect transit time calculations (Stockinger et al., 2015). It  
23 could be shown that spatial and temporal variability of isotope depth profiles can be high  
24 compared to soil moisture profiles. Currently, in-situ measurements are limited to measure  
25 one profile at a time. It could be beneficial to setup more than one laser spectrometer or to  
26 find a way for higher measurement frequency to overcome this limitation.

27 Some pitfalls outlined in other studies can be neglected for the present application. For  
28 instance, water vapor mixing ratio dependencies can be corrected for which is necessary if  
29 humidity is low (Sturm and Knohl, 2010; Aemisegger et al., 2012). This can be neglected in  
30 the present study because the water content was maintained within the density of  
31 approximately  $2 - 4 \cdot 10^{16} \text{ molecules cm}^{-3}$  as recommended by Los Gatos Research. However,  
32 it is assumed that small variations will be reflected in the standard deviation of the

1 measurements. Additionally, inference through organic contamination is neglected in this  
2 study. However, if necessary to account for inference recent efforts include calibration  
3 strategies in this regard (Wu et al., 2014).

4 As a measure of accuracy a standard (HLAU) of known isotopic composition was treated as  
5 an unknown sample. The offset between the drift and span corrected value and the known  
6 value of this quality check standard is calculated. Discrepancies might be result from either  
7 drift that could not be corrected for or device specific properties affected by environmental  
8 conditions. An exhausted reservoir is unlikely at the point because the standard container  
9 were sealed to prevent evaporation.

10 The analytical precision of each sample is determined from the standard deviation of  
11 repetitive measurements. This value might reflect the uncertainty related to the measurement  
12 cycle and a potentially exploited reservoir (see table 2). These values are comparable to other  
13 in-situ studies (see Volkmann & Weiler (2013)). Besides, the analytical error for soil water  
14 extraction in the laboratory especially for very dry soils can be 3 and 5 times higher for  $^{18}\text{O}$   
15 and  $^2\text{H}$  respectively (see Königer et al., 2011). Hence the analytical error is lower for the in-  
16 situ approach.

### 17 **Comparison with destructive sampling**

18 Results of the first field campaign demonstrates good agreement of the isotope depth profiles  
19 between different methods for lower parts but also a divergence in the top 15 cm. This could  
20 be caused by several reasons. An incomplete extraction of water will result in depleted  
21 isotope values of the extracted water. However, this is unlikely for fine sand with very low  
22 matrix potential and very low abundance of fine pores since the cryogenic vacuum extraction  
23 does extract the entire water in sandy soils (Königer et al., 2011). While measuring with the  
24 soil gas probe in a very coarse material atmospheric vapor or even vapor from other parts of  
25 the soil can lead to a mixed sample. However, the extracted air volume is very low and a  
26 divergence of isotope values is only visible within the top 15 cm of the dry profiles (Figure 3,  
27 left and center). Evaporation is reflected in the deuterium excess ( $d_{\text{ex}}$ ) (Figures 5 and 6) and  
28 could be enhanced by the uptake of water vapor through the measurement. However,  
29 enrichment caused by the uptake of air through the measurement is not visible for deeper  
30 parts of profile E1.2 which is very dry as well. Hence, arguing with low water contents would  
31 suggest to have enriched values for deeper parts of the vegetated profile. However this is not  
32 observed at the vegetated plot where soil water contents are below 1% throughout the profile.



1 (Figure 3, center). Therefore it might be rather attributed to kinetic processes because vapor  
2 transport (evaporation) will be higher at shallow depths (Braud et al., 2009). Beside this fact,  
3 it has to be noted, that destructive sampling was conducted one day after the in-situ  
4 measurements because it was assumed that the isotope profiles are in steady state (Barnes and  
5 Allison, 1988). Therefore another explanation can be that high temperature and low humidity  
6 during the day causes a dry out of the top layer due to vapor transport into the atmosphere.  
7 During the night, temperatures decrease and relative humidity increases. Low soil water  
8 contents and a back diffusion of vapor into the upper part of the soil might cause  
9 condensation, affect isotope values (Rothfuss et al., 2015) and can significantly increase soil  
10 water content (Henschel et al., 2008) and might deplete isotope values of the remaining soil  
11 water within that upper layer. In a numerical study it was already shown that diurnal  
12 variations of evaporation can be large depending on the energy budget at the surface but the  
13 influence on isotope concentrations needs to be further investigated especially under field  
14 conditions (Braud et al., 2005).

15 Differences between the two sites of the first field campaign are small regarding the shape of  
16 the isotope depth profiles. **In addition, the evaporating front and the calculated evaporation**  
17 **rates using eq.4 and 5 are similar for both sites.** Because of the litter layer and the shaded  
18 nature of plot E1.2 it could be expected that less evaporation takes place and hence less  
19 enrichment and a lower deuterium excess would appear for the in-situ measurement (Figure ).  
20 However, this is not visible and suggests humidity to be the main driver for isotopic  
21 enrichment as demonstrated in a numerical study by Braud et al. (2005). Interestingly, the  
22 water contents suggest root water uptake at sites with high shrub density even to values as low  
23 as 0.5 % which can be of advantage for competition with other surrounding species.  
24 Depending on uptake rates this can affect infiltration amounts between wet spells, if a higher  
25 storage deficit in the soil has to be satisfied. Beside this, a dense root network in the upper 10  
26 cm suggests that small rain events will be utilized by these plants. It is likely that even small  
27 amounts of water through dew deposition are accessible to plants (Agam and Berliner, 2006).

28 In contrast to the profiles of the first campaign the rain influenced profile E2.7 doesn't show  
29 such a divergence in the top layer. As shown in Figure 5 the deuterium excess indicates that  
30 precipitation water is dominating. Good agreement is found in the top layer for both isotopes.  
31 Mixing with atmospheric vapor might be negligible considering the high soil water contents.  
32 Destructive sampling was done directly before the in-situ measurement started. It has to be

1 noted that, in-situ measurements at 10 cm depth were done 90 min after the destructive  
2 sampling was conducted. In-situ measurements at 30 cm were conducted even 120 min later.  
3 Hence differences can be caused by the time lag between destructive sampling and in-situ  
4 measurement. Another possibility could be non-equilibrium fractionation or condensation due  
5 to vapor transport induced by temperature changes. Values of  $\delta^2\text{H}_I$  below 30 cm are more  
6 enriched compared to  $\delta^2\text{H}_C$ . Therefore, observed differences between  $\delta^2\text{H}_I$  and  $\delta^2\text{H}_C$  for profile  
7 E2.7 (Figure , right) might be attributed to the exchange between the evaporation depleted  
8 vapor that was transported from the deeper part (30 cm to 50cm) to shallower depth (12.5 cm  
9 and 25 cm) due lower saturated water vapor pressure at shallower depth. The movement of  
10 water vapor is following temperature cycles if the saturation vapor pressure of soil air is  
11 similar over depth. In contrast, if the soil air has a vapor pressure deficit there will be a  
12 transfer of vapour towards the zone of higher vapor pressure deficit, which can be  
13 independent of temperature gradients as described in Abramova, (1969).

14 Values for in-situ measurements and cryogenic extraction fall on evaporation lines which are  
15 similar in slope, when the top part of the dry profiles is excluded. The outliers in the top-right  
16 area and those above the LMWL of the  $\delta^2\text{H}$  vs.  $\delta^{18}\text{O}$  plot (Fig. 5) are from the top 12.5 cm of  
17 the profiles. As discussed earlier, kinetic effects and diurnal variations in evaporation or  
18 condensation due to strong temperature changes are not yet fully understood. The interaction  
19 between soil water potential, relative humidity and isotope fractionation is an additional  
20 challenge for future research. **Examples to account for these problems can be found in**  
21 **Soderberg et al., 2012 and Wilson et al., 1997.**

22 **Another possibility for a change in isotopic composition at shallower depth can be hydraulic**  
23 **lift. In this case water from deeper soil layers with lower water potential can move through**  
24 **the root system to soil layers with high water potential (Dawson et al., 1993). The dense root**  
25 **mat of fine roots observed in the lower part of the soil profile together with very low water**  
26 **contents and the differences between the isotope depth profiles could be an indicator for this**  
27 **process. However, the measurement of soil physical properties, stable isotopes of soil water**  
28 **and xylem covering the diurnal cycle would be necessary to distinguish between either vapor**  
29 **back diffusion or hydraulic redistribution. A better understanding and separation of these**  
30 **processes will improve water balance approaches and hence recharge estimations.**

31 **The presented approach is in agreement with most isotope based partitioning studies. Those**  
32 **suggest a contribution of transpiration of more than 70 % to the total evapotranspiration flux**

1 (Sutanto et al., 2014). In addition the findings from field campaign one showed that the  
2 development of the evaporation profiles appeared to be independent of leaf / vegetation cover.  
3 Based on the data and calculation of this study it appears that soil cover might be of minor  
4 importance for long term soil evaporation quantities.

5

## 6 **Spatio-temporal variability**

7 During the second field campaign information on long term precision and spatio-temporal  
8 variability was investigated. Comparing the quality check standards of the two campaigns the  
9 precision within one series ( $\sigma_{\text{rep}}$ ) of  $\delta^2\text{H}$  is one-third better than the long term accuracy.  
10 However, the accuracy of  $\delta^{18}\text{O}$  is three times greater than the mean precision (Table 2). This  
11 can likely be improved by utilizing a more sophisticated technical setup e.g. temperature  
12 controlled conditions, standard preparation and frequent cleaning of the probes. Another  
13 reason could be the difference in the physical properties of the probe pores such as the  
14 diffusivity to gas (Merlivat et al., 1979). However, the precision appears to be sufficient to  
15 monitor processes of a diurnal time scale which is comparable to other systems, e.g.,  
16 Volkmann and Weiler et al. (2013) present values of 2.6 ‰ and 0.38 ‰ for  $\delta^2\text{H}$  and  $\delta^{18}\text{O}$ ,  
17 respectively.

18 The boundary conditions of the second field campaign caused a quite heterogeneous pattern  
19 regarding both the development of the moisture front and the isotope depth profiles. It can be  
20 observed how the infiltrating water develops under evaporation with light intermitted rainfall  
21 events. This is reflected in both the shape of isotope depth profiles of the three transects and  
22 the standard deviations within one transect (Figure 6). Other studies showed similar patterns  
23 in the context of a numerical experiment (Singleton et al., 2004). The first transect (Figure 6,  
24 Transect 1) has variable isotope values throughout the whole depth. The isotope depth profile  
25 of transect one shows maxima and minima of isotope values which appears with a similar  
26 shape as a profile in a humid climate. **This kind of layering is commonly used in humid**  
27 **regions to determine transit times of unsaturated zone water where precipitation has seasonal**  
28 **different isotopic composition (Coplen et al., 2000; Lee et al., 2007).** However, here it is  
29 attributed to variations in rainfall composition and infiltration patterns on a much smaller time  
30 scale namely daily. Zimmermann et al., (1967) previously described that isotopically distinct  
31 rain that is consecutively infiltrating into the soil will move downward distinguishable by a  
32 boundary between older rainwater below and younger water above. Hence, the most depleted

1 values found at 20 cm and 50 cm (Figure 6, Transect 1) might correspond to certain rain  
2 events which would not emerge from the soil moisture measurements alone. These depleted  
3 zones are not visible in the other transects which are possibly overprinted by vapor transport  
4 processes and evaporation.

5 Short time after rain the top part of the evaporation profile (Transect 1) was considerably  
6 displaced as theoretically described by Allison et al., (1984). Variations of isotope values are  
7 attenuated with time by vapor phase redistribution (Transect 2) (Fontes et al., 1986) and an  
8 evaporation profile is begins to develop (Transect 3). Further it can be observed that  
9 infiltrating water of small intermittent events compresses the isotope profile (Barnes and  
10 Allison, 1988; Singleton et al., 2004). Therefore the presented in-situ measurements have  
11 great potential to visualize theoretically discussed processes with feasible accuracy under  
12 natural field conditions.

13 Spatial variability of soil moisture is well known (Western et al., 2004). It can be expected  
14 that also stable isotopes will distribute heterogeneous within the unsaturated zone. The  
15 relationship between mean soil moisture and  $\delta^2\text{H}$  does not allow a resilient conclusion  
16 because of the low accuracy. However, it appears that it behaves different to  $\delta^{18}\text{O}$  and soil  
17 moisture as well as  $\delta^{18}\text{O}$  values show a different pattern as soil moisture. This might be  
18 reasonable considering the difference in physical properties of the two isotopologues  
19 (Merlivat, 1978). However, the intention to show isotope depth profiles for each transect with  
20 their standard deviation for isotopes and soil moisture was to show the difference between the  
21 two. The variability within the isotope depth profiles shows a much more heterogeneous  
22 pattern than that of the soil moisture data. Dawson et al., (2002) discussed the isotopic  
23 composition of different carbon and water pools. Since soil respiration will equilibrate with  
24 the abundant soil water this might cause additional changes of the isotopic composition in soil  
25 pore water.

## 26 **Potentials, limitations and future research**

27 From a technical point of view the reliability of the system depends upon each used  
28 component (i.e. valves, computer, interface etc). The bottleneck of in-situ systems in terms of  
29 maintenance are the membrane probes, the air supply and the standard container. The  
30 membrane pores might clog in fine textured soils and will need to be cleaned; the dry air  
31 supply is limited on the size of tank provided. It is recommendable to refresh the standards in

1 the containers at least every two days to avoid misleading results. However, this will depend  
2 on the size of the container and the water content of the prepared standard.

3 Condensation within the sample system can lead to unreliable data. This can be either  
4 prevented by heating the sample lines, flushing the sample lines with dry air or sufficient  
5 dilution of the sample. Hence, under conditions where the ambient temperature is significant  
6 warmer than the soil temperature a simple valve controlled membrane inlet will be sufficient  
7 for an indirect determination of isotopes in unsaturated zone or saturated zone water. During  
8 day time this is the case at the presented study site, but changes drastically over night as  
9 described.

10 Dilution of the vapor concentration can be done by providing dry gas at the other end of the  
11 available probes. In that case of pure diffusion sampling the maximum dilution rate under  
12 absolute humidity is controlled by the length of the probe, their diffusion properties, the flow  
13 velocity and the temperature at depth. The flow velocity can be different depending on the  
14 laser spectrometer that is used. Adding a mixing chamber at the head of the probe has the  
15 distinct advantage of additional mixing directly before the vapor enters the sample line  
16 (Volkman and Weiler, 2014). This leads to independence on flow velocity, probe length and  
17 membrane diffusion properties in terms of water content. However, under very dry conditions  
18 it might be useful to increase probe length for an increase of resolution, since the soil volume  
19 around the probe affected by the measurement will be reduced.

20 Another critical point is the long term application of membrane based methods. The pore  
21 space of the probes can be altered over time which might increase the memory effect of the  
22 system. Further, the calibration of the in-situ methods of Volkman and Weiler (2013) and  
23 this study used prior oven dried substrate for the calibration. Though it is assumed that all  
24 water is evaporated from the oven dried substrate and only the added standard water will be  
25 measured afterwards. The same assumption is made using the equilibration bag method if the  
26 standards are treated in the same way as described. A direct comparison of the cryogenic  
27 vacuum extraction with a membrane based in-situ measurement showed that this calibration  
28 procedure is applicable for fine sand. However, it will probably lead to insufficient data  
29 applying this calibration procedure to soil samples with finer texture, especially if clay and/or  
30 salt contents are high.

## 1 **5 Conclusion**

2 **Summing up, to prevent the collection of insufficient data applying an in situ approach one**  
3 **has to carefully consider the applied calibration procedure depending on the research question**  
4 **and the soil type. In addition, there is a trade-off between technical effort, control setup, probe**  
5 **type, environmental conditions and costs.**

6 The present study demonstrates that high resolution in-situ sampling of stable isotopes in the  
7 unsaturated zone is feasible. In-situ measurements can be applied with minimal technical  
8 effort for remote applications. They further show good agreement with values derived from  
9 cryogenic soil water extractions. Differences between the two methods are predominantly  
10 within the given accuracies of the methods. Divergence in the upper soil layer between in-situ  
11 and destructive sampling suggest enhanced soil-atmosphere interactions, kinetic processes  
12 due to high evaporation rates or hydraulic redistribution. However, evaporation induced by  
13 the measurement procedure needs further investigation for very low water contents to reduce  
14 limitations. In addition, low humidity in relation to soil water potential and isotope  
15 fractionation needs further investigation. Long term accuracy within the presented campaigns  
16 is about two times lower for  $\delta^2\text{H}$  and three times for  $\delta^{18}\text{O}$  than for the short term precision of  
17 each profile. This can possibly be improved by a better temperature control of the analyser or  
18 temperature compensated devices if available.

19 The presented in-situ measurements have great potential to investigate transient processes  
20 within the unsaturated zone of semi-arid environments. This has not been possible to study  
21 until field deployable laser spectrometer and in-situ techniques became available. The  
22 determination of water stable isotopes in the unsaturated zone directly in the field allows  
23 monitoring transient processes which would not be possible with destructive sampling  
24 strategies. This creates new possibilities to the design of tracer experiments with water of  
25 different isotopic composition as conservative tracer. However, this is limited by the  
26 measurement frequency of the provided system which is now at least able to capture diurnal  
27 processes with the presented vertical resolution. In addition, a much higher spatial resolution  
28 can be achieved with much lower time consumption compared to conventional approaches.  
29 The proposed technique offers the possibility to investigate unsolved questions regarding soil  
30 atmosphere interactions such as water vapor intrusion and transport plus effects of diurnal  
31 evaporation cycling on isotope depth profiles. Strategies of plant root water uptake in water  
32 scarce environments are not yet fully understood as well as the role of water vapor transport.

1 Determination of fractionation factors between water vapor and liquid water will also require  
2 advanced calibration procedures. Besides, properties of the membrane may cause  
3 fractionation and might require characterization for alternative calibration procedures.  
4 Therefore future research on in-situ methods should investigate different calibration  
5 procedures in more detail. Pure vapor standards should be tested against standards prepared  
6 with prior dried soil with different water content. Additionally, the direct determination of soil  
7 water using extraction methods should be further studied for different soils and compared to  
8 the available equilibration and in-situ methods. This will give more insight into the  
9 applicability of an in-situ approach under various climatic conditions and for different soil  
10 types.

11

## 1 **Acknowledgements**

2 This work was partly funded by the German Federal Ministry for Education and Research  
3 (BMBF) within the SASSCAL project (South African Science and Service Center for Climate  
4 Change, Agriculture and Landuse) under contract number 01LG1201L. We wish to thank our  
5 colleagues Martin Quinger (BGR), Christoph Lohe (BGR), Shoopi Ugulu, and Wilhelm  
6 Nuumbembe from University of Namibia, Windhoek, Namibia. Laboratory work was  
7 supported by Jürgen Rausch and Lisa Brückner which is highly acknowledged. Also  
8 appreciated is the technical support of Axel Lamparter, Marc Brockmann, Erik Lund and  
9 Salome Krüger as well as Chris Gabrielli for reviewing the article.

10



## 1 **6 References**

- 2 Abramova, M. M.: Movement of moisture as a liquid and vapour in soils of semi-deserts,  
3 *Internat. Assoc. Sci. Hydrol., Proc. Wageningen Symposium (83)*, 781–789, 1969.
- 4 Adomako, D., Maloszewski, P., Stumpp, C., Osae, S., and Akiti, T. T.: Estimating  
5 groundwater recharge from water isotope ( $\delta^2\text{H}$ ,  $\delta^{18}\text{O}$ ) depth profiles in the Densu River  
6 basin, Ghana, *Hydrological Sciences Journal*, 55 (8), 1405–1416,  
7 doi:10.1080/02626667.2010.527847, 2010.
- 8 Aemisegger, F., Sturm, P., Graf, P., Sodemann, H., Pfahl, S., Knohl, A., and Wernli, H.:  
9 Measuring variations of  $\delta^{18}\text{O}$  and  $\delta^2\text{H}$  in atmospheric water vapour using two commercial  
10 laser-based spectrometers: an instrument characterisation study, *Atmos. Meas. Tech.* (5),  
11 1491–1511, doi:10.5194/amt-5-1491-2012, 2012.
- 12 Agam, N. and Berliner, P. R.: Dew formation and water vapor adsorption in semi-arid  
13 environments - A review, *Journal of Arid Environments* (4), 572–590,  
14 doi:10.1016/j.jaridenv.2005.09.004, 2006.
- 15 Allison, G. B., Barnes, C. J., and Hughes M.W.: The distribution of deuterium and  $^{18}\text{O}$  in dry  
16 soils 2. Experimental, *Journal of Hydrology* (64), 377–397, 1983.
- 17 Allison G.B., Barnes, C. J., Hughes M.W., and Leaney, F. W.: Effect of climate and  
18 vegetation on oxygen-18 and deuterium profiles in soils, *Int. Symp. Iso. Hydrol. Water*  
19 *Resour. Dev.*, 105–123, 1984.
- 20 Allison G.B., Barnes, C.J., Hughes M.W.: Estimation of evaporation from the normally "dry"  
21 lake frome in south Australia, *Journal of Hydrology* (78), 229–242, 1985.  
22
- 23 Allison, G. B., Colin-Kaczala A.F., and Fontes Ch.J.: Measurement of Isotopic Equilibrium  
24 between Water, Water Vapour and Soil  $\text{CO}_2$  in Arid Zone Soils, *Journal of Hydrology* (95),  
25 131–141, 1987.
- 26 Allison, G. B., Gee, G., and and Tyler, S. W.: Vadose-Zone Techniques for Estimating  
27 Groundwater recharge in Arid and Semiarid Regions, *Soil Sci. Soc. Am.* (58), 6–14, 1994.
- 28 Allison, G. B. and Hughes, M. W.: The use of natural tracers as indicators of soil-water  
29 movement in a temperate semi-arid region, *Journal of Hydrology* (60), 157–173, 1983.

1 Altuhafi, F., O'Sullivan, C., and Cavarretta, I.: Analysis of an Image-Based Method to  
2 Quantify the Size and Shape of Sand Particles, *J. Geotech. Geoenviron. Eng.*, 139 (8), 1290–  
3 1307, doi:10.1061/(ASCE)GT.1943-5606.0000855, 2013.

4 Barnes, C. J. and Allison, G. B.: The distribution of deuterium and  $^{18}\text{O}$  in dry soils: 1. Theory,  
5 *Journal of Hydrology* (60), 141–156, 1983.

6 Barnes, C. J. and Allison, G. B.: Tracing of Water Movement in the unsaturated zone using  
7 stable isotopes of hydrogen and oxygen, *Journal of Hydrology* (100), 143–176, 1988.

8 Berman, Elena S. F., Gupta, M., Gabrielli, C., Garland, T., and McDonnell, J. J.: High-  
9 frequency field-deployable isotope analyzer for hydrological applications, *Water Resour.*  
10 *Res.*, 45 (10), doi:10.1029/2009WR008265, 2009.

11 Braud, I., Bariac, T., Biron, P., and Vauclin, M.: Isotopic composition of bare soil evaporated  
12 water vapor. Part II: Modeling of RUBIC IV experimental results, *Journal of Hydrology*, 369  
13 (1-2), 17–29, doi:10.1016/j.jhydrol.2009.01.038, 2009.

14 Braud, I., Bariac, T., Vauclin, M., Boujamlaoui, Z., Gaudet, J. P., Biron, P., and Richard, P.:  
15 SiSPAT-Isotope, a coupled heat, water and stable isotope ( $\text{HDO}$  and  $\text{H}_2^{18}\text{O}$ ) transport model  
16 for bare soil. Part II. Evaluation and sensitivity tests using two laboratory data sets, *Journal of*  
17 *Hydrology* (309), 301–320, doi:10.1016/j.jhydrol.2004.12.012, 2005.

18 Caldwell, M. M., Dawson, T. E., and Richards, J. H.: Hydraulic lift: consequences of water  
19 efflux from the roots of plants, *Oecologia*, 113 (2), 151–161, doi:10.1007/s004420050363,  
20 1998.

21 Christelis, G. and Struckmeier, W.: Groundwater in Namibia: an explanation to the  
22 Hydrogeological Map, 2011st ed., 2001.

23 Clark, I. D. and Fritz, P.: *Environmental Isotopes in Hydrogeology*, Lewis Publishers, 1997.

24 Craig, H.: Isotopic Variations in Meteoric Waters, *American Association for the*  
25 *Advancement of Science* (133), 1961.

26 Coplen, T., Herczeg, A., and Barnes, C.: Isotope Engineering—Using Stable Isotopes of the  
27 Water Molecule to Solve Practical Problems, in: *Environmental Tracers in Subsurface*  
28 *Hydrology*, Springer US, 79-110, doi: 10.1007/978-1-4615-4557-6\_3, 2000.

29 Dansgaard, W.: Stable isotopes in precipitation, *Tellus* (4), 1964.

1 Dawson, T. E.: Hydraulic lift and water use by plants: implications for water balance,  
2 performance and plant-plant interactions, *Oecologia* (95), 565–574, 1993.

3 Dawson, T. E.: Determining water use by trees and forests from isotopic, energy balance and  
4 transpiration analyses: the roles of tree size and hydraulic lift, *Tree Physiology* (16), 263–272,  
5 1996.

6 Dawson, T. E. and Ehleringer, J. R.: Streamside trees that do not use stream water, *Nature*,  
7 350 (6316), 335–337, 1991.

8 Dawson, T. E., Mambelli, S., Plamboeck, A. H., Templer, P. H., and TU, K. P.: Stable  
9 Isotopes in Plant Ecology, *Annu. Rev. Ecol. Syst.*, 33 (1), 507–559,  
10 doi:10.1146/annurev.ecolsys.33.020602.095451, 2002.

11

12 Dincer, T., Al-Mugrin, A., and Zimmermann, U.: Study of the infiltration and recharge  
13 through the sand dunes in arid zones with special reference to the stable isotopes and  
14 thermonuclear tritium, *Journal of Hydrology*, 23 (1-2), 79–109, doi:10.1016/0022-  
15 1694(74)90025-0, 1974.

16 Dragnich, P. A., Dungca, A. C., Pedleton Noah, L., and Tracy, A. R.: The Cuvelai-Etосha  
17 Basin Management Approach; Assessing water resources management in the Iishana sub-  
18 basin ), 2004.

19 Dubbert, M.; Cuntz, M. M.; Piayda, A.; Maguàs; Werner, C.: Partitioning evapotranspiration - Testing  
20 the Craig and Gordon model with field measurements of oxygen isotope ratios of evaporative fluxes  
21 (496), 142–153, doi:10.1016/j.jhydrol.2013.05.033, 2013.

22 Ehleringer, J. R. and Dawson, T. E.: Water uptake by plants: perspectives from stable isotope  
23 composition, *Plant Cell Environ*, 15 (9), 1073–1082, doi:10.1111/j.1365-  
24 3040.1992.tb01657.x, 1992.

25 Fontes, J., Yousfi, M., and Allison, G. B.: Estimation of long-term, diffuse groundwater  
26 discharge in the northern Sahara using stable isotope profiles in soil water, *Journal of*  
27 *Hydrology* (86), 315–327, 1986.

28 Garvelmann, J., Külls C., and Weiler M.: A porewater-based stable isotope approach for the  
29 investigation of subsurface hydrological processes, *Hydrol. Earth Syst. Sci.* (16), 631–640,  
30 doi:10.5194/hess-16-631-2012, 2012.

1 Gazis, C. and Feng, X.: A stable isotope study of soil water: evidence for mixing and  
2 preferential flow paths, *Geoderma*, 119 (1-2), 97–111, doi:10.1016/S0016-7061(03)00243-X,  
3 2004.

4 Henschel, J. R. and Seely, M. K.: Ecophysiology of atmospheric moisture in the Namib  
5 Desert., *Atmospheric Research*, 87 (87), 362–368, doi:10.1016/j.atmosres.2007.11.015,  
6 2008.

7 Herbstritt, B., Grahler B., and Weiler M.: Continuous in situ measurements of stable isotopes  
8 in liquid water, *Water Resour. Res.* (48), doi:10.1029/2011WR011369, 2012.

9 Herczeg, A. L., & Leaney, F. W. (2011). Review: environmental tracers in arid-zone  
10 hydrology. *Hydrogeology Journal*, 19(1), 17-29.

11 Kelln, C., Wassenaar L.I., and Hendry, M. J.: Stable Isotopes ( $\delta^{18}\text{O}$ ,  $\delta^2\text{H}$ ) of Pore Waters in  
12 Clay-Rich Aquitards: A Comparison and Evaluation of Measurement Techniques, 108–116,  
13 2001.

14 Kendall, C. and McDonnell, J. J.: *Isotopes in catchment hydrology*, Elsevier, 2012.

15 Koeniger, P., Gaj, M., Beyer, M., and Himmelsbach, T.: Review on soil water stable isotope  
16 based groundwater recharge estimations, *Hydrol. Process.*, submitted.

17 Koeniger, P., Marshall, J. D., Link, T., and Mulch, A.: An inexpensive, fast, and reliable  
18 method for vacuum extraction of soil and plant water for stable isotope analyses by mass  
19 spectrometry, *Rapid Commun. Mass Spectrom.*, 25 (20), 3041–3048, doi:10.1002/rcm.5198,  
20 2011.

21 Lindenmaier, F. and Christelis, G. (Eds.): *Groundwater for the North of Namibia: Summary  
22 Report of Activities of Phase I, Exploration of Ohangwena II Aquifer and Preliminary Isotope  
23 Study, Volume 1a*, Windhoek, 2012.

24 Lindenmaier, F., Lohe C., and Quinger M.: *Groundwater for the North of Namibia: Executive  
25 Summary Phase I*, Windhoek, 2014.

26 Lee, K.S., Kim, J.M., Lee, D.-R., Kim, Y., and Lee, D.: Analysis of water movement through  
27 an unsaturated soil zone in Jeju Island, Korea using stable oxygen and hydrogen isotopes,  
28 *Journal of Hydrology*, 345 (3-4), 199–211, doi:10.1016/j.jhydrol.2007.08.006, 2007.

29 McDonnell, J. J.: The two water worlds hypothesis: ecohydrological separation of water  
30 between streams and trees?, *WIREs Water* (1), 323–329, doi:10.1002/wat2.1027, 2014.

1 Mendelsohn, J., Jarvis A., Robertson T., Mendelsohn, J., Jarvis, A., and Robertson, T.: A  
2 Profile and Atlas of the Cuvelai - Etosha Basin, RAISON; Gondwana Collection, Windhoek,  
3 Namibia, 172 // 170, 2013.

4 Merlivat L.: Molecular diffusivities of H<sub>2</sub><sup>16</sup>O, HD<sup>16</sup>O, and H<sub>2</sub><sup>18</sup>O in gases, The Journal of  
5 chemical Physics (69), doi:10.1063/1.436884, 1978.

6

7 Mueller, M. H., Alaoui, A., Kuells, C., Leistert, H., Meusburger, K., Stumpp, C., Weiler, M.,  
8 and Alewell, C.: Tracking water pathways in steep hillslopes by δ<sup>18</sup>O depth profiles of soil  
9 water, Journal of Hydrology (519), 340–352, doi:10.1016/j.jhydrol.2014.07.031, 2014.

10 Or, D., Lehmann, P., Shahraeeni, E., & Shokri, N. (2013). Advances in soil evaporation  
11 physics—A review. *Vadose Zone Journal*, 12(4).

12 Orłowski, N., Frede, H.-G., Brüggemann, N., and Breuer, L.: Validation and application of a  
13 cryogenic vacuum extraction system for soil and plant water extraction for isotope analysis, J.  
14 Sens. Sens. Syst. (2), 179–193, doi:10.5194/jsss-2-179-2013, 2013.

15 Rambo, J., Lai C-T., and Farlin J.: On-Site Calibration for High Precision Measurements of  
16 Water Vapor Isotope Ratios Using Off-Axis Cavity-Enhanced Absorbtion Spectroscopy,  
17 Journal of Atmospheric and Oceanic Technology (28), 1448–1457, 2011.

18 Richard, P. and Shoemaker, C. A.: A Comparison of Chemical and Isotopic Hydrograph  
19 Separation, Water Resour. Res. (22(10)), 1444–1454, 1986.

20 Rothfuss, Y., Vereecken, H., and Brüggemann, N.: Monitoring water stable isotopic  
21 composition in soils using gas-permeable tubing and infrared laser absorption spectroscopy,  
22 Water Resour. Res., 49 (6), 3747–3755, doi:10.1002/wrcr.20311, 2013.

23 Rothfuss, Y., Merz, S., Vanderborght, J., Hermes, N., Weuthen, A., Pohlmeier, A.,  
24 Vereecken, H., and Brüggemann, N.: Long-term and high frequency non-destructive  
25 monitoring of water stable isotope profiles in an evaporating soil column, Hydrol. Earth Syst.  
26 Sci. Discuss., 12, 3893-3918, doi:10.5194/hessd-12-3893-2015, 2015.

27 Saxena, R. K.: Oxygen-18 fractionation in nature and estimation of groundwater recharge,  
28 Uppsala University, Department of Physical Geography, Divisidon of Hydrology, 1987.

1 Scanlon, B. R., Healy, R. W., and Cook, P. G.: Choosing appropriate techniques for  
2 quantifying groundwater recharge, *Hydrogeology Journal*, 10 (1), 18–39,  
3 doi:10.1007/s10040-001-0176-2, 2002.

4 Schack-Kirchner, H., Hildebrand, E. E., and Wilpert, K. von: Ein konvektionsfreies  
5 Sammelsystem für Bodenluft, *Pflanzenernährung und Bodenkunde* (156), 307–310, 1993.

6 Singleton, M. J., Sonnenthal, E.L, Conrad, M.E., DePaolo, D., and Gee, G. W.: Multiphase  
7 Reactive Transport Modeling of Seasonal Infiltration Events and Stable Isotope Fractionation  
8 in Unsaturated Zone Pore Water and Vapor at the Hanford Site, *Vadose Zone Journal* (3),  
9 775–785, 2004.

10 Sklash, M. G. and Farvolden, R. N.: The role of groundwater in storm runoff., *Journal of*  
11 *Hydrology* (43), 45–65, 1979.

12 Soderberg, K., Good, S. P., Wang, L., and Caylor, K.: Stable Isotopes of Water Vapor in the  
13 Vadose Zone: A Review of Measurement and Modeling Techniques, *Vadose Zone Journal*,  
14 11 (3), 0, doi:10.2136/vzj2011.0165, 2012.

15 Sutanto, S. J., van den Hurk, B., Dirmeyer, P. A., Seneviratne, S. I., Röckmann, T., Trenberth,  
16 K. E., Blyth, E. M., Wenninger, J., and Hoffmann, G.: HESS Opinions "A perspective on  
17 isotope versus non-isotope approaches to determine the contribution of transpiration to total  
18 evaporation", *Hydrol. Earth Syst. Sci.*, 18 (8), 2815–2827, doi:10.5194/hess-18-2815-2014,  
19 2014.

20 Sprenger, M., Volkmann, T. H. M., Blume, T., and Weiler, M.: Estimating flow and transport  
21 parameters in the unsaturated zone with pore water stable isotopes, *Hydrol. Earth Syst. Sci.*  
22 *Discuss.*, 11 (10), 11203–11245, doi:10.5194/hessd-11-11203-2014, 2014.

23 Steenhuis, T. S., Rivera, J. C., Hernández, C., Walter, M. T., Bryant, R. B., and Nektarios, P.:  
24 Water repellency in New York state soils, *International Turfgrass Society* (9), 624–625, 2001.

25 Stockinger, M.P.; Lücke, A.; McDonnell, J.J.; Diekkrüger, B.; Vereecken, H.; Bogaen, H.R.  
26 (2015): Interception effects on stable isotope driven streamwater transit time estimates.  
27 *Geophys. Res. Lett.* 42 (13), S. 5299–5308. DOI: 10.1002/2015GL064622.

28 Stumpp, C. and Maloszewski, P.: Quantification of preferential flow and flow heterogeneities  
29 in an unsaturated soil planted with different crops using the environmental isotope  $\delta^{18}\text{O}$ ,  
30 *Journal of Hydrology*, 394 (3-4), 407–415, doi:10.1016/j.jhydrol.2010.09.014, 2010.

- 1 Sturm, P. and Knohl, A.: Water vapor  $\delta^2\text{H}$  and  $\delta^{18}\text{O}$  measurements using off-axis integrated  
2 cavity output spectroscopy, *Atmos. Meas. Tech.*, 3 (1), 67–77, doi:10.5194/amt-3-67-2010,  
3 2010.
- 4 Skrzypek, G., Mydłowski, A., Dogramaci, S., Hedley, P., Gibson, J. J., & Grierson, P. F.  
5 (2015). Estimation of evaporative loss based on the stable isotope composition of water using  
6 Hydrocalculator. *Journal of Hydrology*, 523, 781-789.
- 7 Tetzlaff, D., Soulsby, C., Waldron, S., Malcolm, I. A., Bacon, P. J., Dunn, S. M., Lilly, A.,  
8 and Youngson, A. F.: Conceptualization of runoff processes using a geographical information  
9 system and tracers in a nested mesoscale catchment, *Hydrol. Process.*, 21 (10), 1289–1307,  
10 doi:10.1002/hyp.6309, 2007.
- 11 van Geldern, R. and Barth, J. A.: Optimization of instrument setup and post-run corrections  
12 for oxygen and hydrogen stable isotope measurements of water by isotope ratio infrared  
13 spectroscopy (IRIS), *Limnol. Oceanogr. Methods* (10), 1024–1036,  
14 doi:10.4319/lom.2012.10.1024, 2012.
- 15 Volkmann, T. and Weiler, M.: Continual in-situ monitoring of pore water stable isotopes,  
16 *Hydrol. Earth Syst. Sci.* (18), 1819–1833, doi:10.5194/hess-18-1819-2014, 2013.
- 17 Walker, G. R., Woods, P. H., and Allison, G. B.: Interlaboratory comparison of methods to  
18 determine the stable isotope composition of soil water, *Chemical Geology*, 111 (1-4), 297–  
19 306, doi:10.1016/0009-2541(94)90096-5, 1994.
- 20 Wang, L., Caylor, K., and Dragoni, D.: On the calibration of continuous, high-precision  $\text{d}^{18}\text{O}$   
21 and  $\text{d}^2\text{H}$  measurements using an off-axis integrated cavity output spectrometer (23), 530–536,  
22 2009.
- 23 Wang, L., Good, S. P., Caylor, K. K., and Cernusak, L. A.: Direct quantification of leaf  
24 transpiration isotopic composition, *Agricultural and Forest Meteorology* (154-155), 127–135,  
25 doi:10.1016/j.agrformet.2011.10.018, 2012.
- 26 Wassenaar, L. I., Hendry, M. J., Chostner V.L., and Lis G.P.: High Resolution Pore Water  $^2\text{H}$   
27 and  $^{18}\text{O}$  Measurements by  $\text{H}_2\text{O}_{(\text{liquid})}\text{H}_2\text{O}_{(\text{vapor})}$  Equilibration Laser Spectroscopy,  
28 *Environmental Science and Technology* (42), 9262–9267, 2008.

- 1 West, A. G., Patrickson, S.J., Ehleringer, J.R.: Water extraction times for plant and soil  
2 materials used in stable isotope analysis, *Rapid Commun. Mass Spectrom.* (20): 1317-1321,  
3 2006.
- 4 Western, Andrew W.; Zhou, Sen-Lin; Grayson, Rodger B.; McMahon, Thomas A.; Blöschl,  
5 Günter; Wilson, David J. (2004): Spatial correlation of soil moisture in small catchments and  
6 its relationship to dominant spatial hydrological processes. *Journal of Hydrology* 286 (1-4), S.  
7 113–134. DOI: 10.1016/j.jhydrol.2003.09.014.
- 8 Wilson G.W., Fredlund D.G., and Barbour S.L.: The effect of soil suction on evaporative  
9 fluxes from soil surfaces., *Can. Geotech. Journal* (34), 145–155, 1997.
- 10 Wu, Y., Zhou, H., Zheng, X.-J., Li, Y., and Tang, L.-S.: Seasonal changes in the water use  
11 strategies of three co-occurring desert shrubs, *Hydrol. Process.*, 28 (26), 6265–6275,  
12 doi:10.1002/hyp.10114, 2014.
- 13 Yang Q., Xiao, H., Zhao, L., Zhou, M., and Li, C., Coa, S.: Stable isotope techniques in plant  
14 water sources: a review, *Science in Cold and Arid Regions* (2), 0112–0122, 2010.
- 15 Zimmermann, U., Münnich K.O., and Roether W.: Downward movement of soil moisture  
16 traced by means of hydrogen isotopes, *Geophysical Monograph Series* (11), 1967.



1 **Table 1: Standards used for normalization, drift correction, quality check and preparation of field**  
 2 **standards.**

Abbreviation	Description	$\delta^2\text{H}$ [‰]	$\sigma$	$\delta^{18}\text{O}$ [‰]	$\sigma$
HMER	Hannover sea water	-3.1	$\pm 0.4$	-0.4	$\pm 0.13$
HDES	Hannover distilled water	-55.9	$\pm 0.9$	-8.12	$\pm 0.14$
H LAU	Hannover lauretaner water	-64.6	$\pm 0.6$	-9.73	$\pm 0.10$
HGLA	Hannover glacier water	-152.1	$\pm 0.9$	-20.27	$\pm 0.11$

3  
 4 **Table 2: Values for H LAU (qc) with the corresponding standard deviation of their repetitive**  
 5 **measurements ( $\sigma_{qc}$ ), the mean standard deviation of the repetitive measurements of each measurement**  
 6 **point ( $\sigma_{rep}$ ) and the corresponding values of the cryogenic vacuum extraction ( $\sigma_{cry}$ ) from the campaigns**  
 7 **June / November 2014. Bare plots (B) and vegetated plots (V) were measured.**

ID	Date	Init.Time		$\delta^2\text{H}$ [‰]	$\sigma_{qc}$	$\sigma_{rep}$	$\sigma_{cry}$	$\delta^{18}\text{O}$ [‰]	$\sigma_{qc}$	$\sigma_{rep}$	$\sigma_{cry}$	
E1.1	04.06.2014	09:30:00	B	-60.09	$\pm 5.13$	1.4	3.7	-10.04	$\pm 0.66$	0.7	0.8	
E1.2	04.06.2014	15:30:00	V	-74.96	$\pm 2.83$	3	3.5	-13.16	$\pm 0.01$	0.6	0.6	
					$\pm 3.98$	2.2	3.6		$\pm 0.34$	0.65	0.70	
E2.1	15.11.2014	10:50:00	B	-73.25	$\pm 0.87$	1.17		-10.38	$\pm 0.34$	0.45		
E2.2	16.11.2014	08:00:00	B	-69.83	$\pm 0.99$	1.26		-8.05	$\pm 0.48$	0.35		
E2.3	16.11.2014	13:30:00	V	-71.11	$\pm 0.49$	2.21		-10.29	$\pm 0.14$	0.54		
E2.4	17.11.2014	11:00:00	V	-57.51	$\pm 4.11$	1.72		-8.45	$\pm 0.14$	0.28		
E2.5	18.11.2014	11:00:00	V	-64.82	$\pm 1.86$	1.52		-7.73	$\pm 0.34$	0.28		
E2.6	19.11.2014	07:30:00	B	-75.62	$\pm 1.84$	2.49		-6.81	$\pm 0.81$	0.5		
E2.7	19.11.2014	14:00:00	B	-79.35	$\pm 1.27$	1.93	3.5	-11.62	$\pm 0.36$	0.45	0.45	
E2.8	20.11.2014	11:30:00	V	-25.24	$\pm 2.53$	1.45		-3.68	$\pm 0.25$	0.24		
E2.9	21.11.2014	11:30:00	V	-23.00	$\pm 17.17$	1.74		-15.59	$\pm 4.17$	0.37		
						2.15	1.86	3.57		0.36	0.46	0.62

9  
 10

1

2 **Table 2: Soil water balance derived from stable isotope data.  $z_{ef}$  estimated from a exponential fit to isotope**  
 3 **depth profiles. The contribution of transpiration is the remainder of soil water and hence potentially**  
 4 **available.**

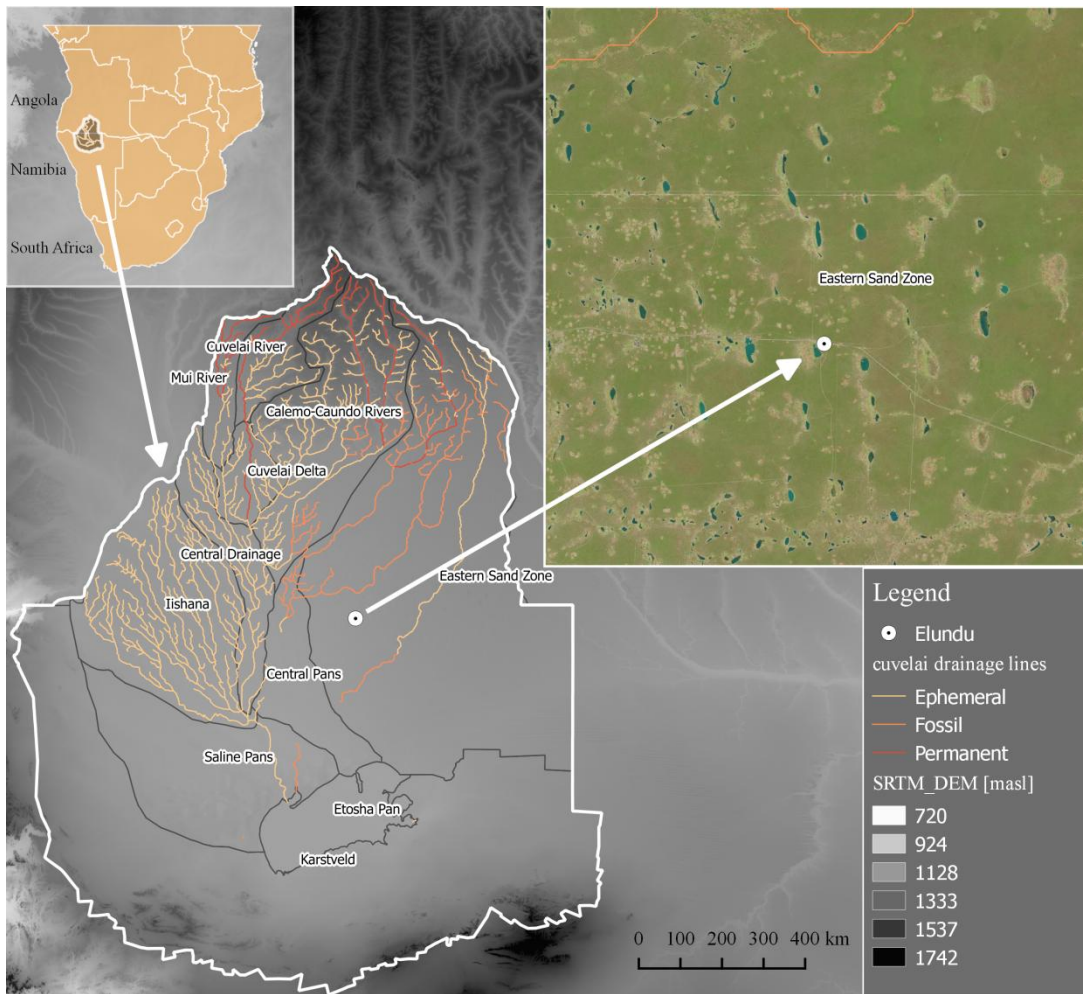
 **$^{18}\text{O}$** 

	$z_{ef}$ [mm]	$\delta_{res}$ [‰]	$\delta_{ef}$ [‰]	E [mm/y]		S [mm]	T [mm/y]		E/T_pot [%]	
				$\Theta:1\%$	$\Theta:7\%$		$\Theta:1\%$	$\Theta:7\%$		
<b>Cryo</b>										
<i>bare</i>	155	-8.2	31.4	150	127	40	465	488	76	79
<i>vegetated</i>	126	-5.2	33	185	156	9.5	460.5	489.5	71	76
Wet	61	-4	6.2	382	323	122	152	220	28	41
<b>In-situ</b>										
<i>bare</i>	111	-6.3	46	202	171	40	453	485	69	74
<i>vegetated</i>	249	-18.3	28.8	93	79	9.5	562	576	86	88
Wet	51	-3.9	7.6	458	387	122	80	156	15	29

 **$^2\text{H}$** 

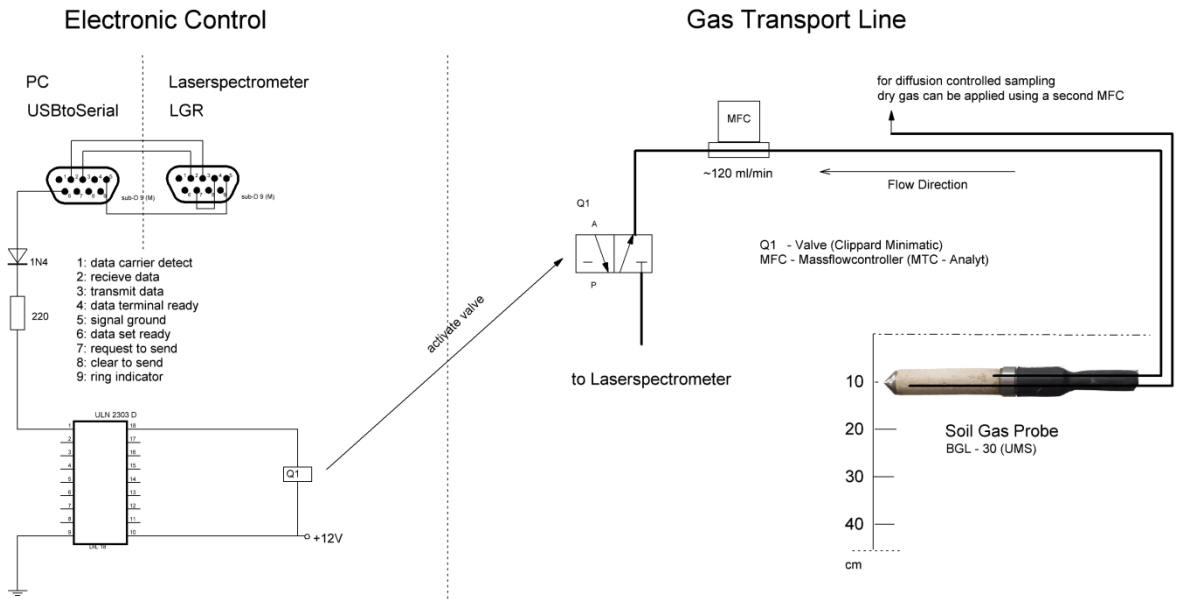
<b>Cryo</b>										
<i>bare</i>	290	-73.4	30.79	79	67	40	537	549	87	89
<i>vegetated</i>	190	-51.8	29.4	111	94	9.5	535.5	552.5	83	85
Wet	68	-21.2	32.5	342	289	122	192	253	36	47
<b>In-situ</b>										
<i>bare</i>	158	-61	82	147	124	40	469	492	76	80
<i>vegetated</i>	145	-46	97	161	136	9.5	485.5	510.5	75	79
Wet	52	-24.4	34	449	380	122	89	163	17	30

5



1  
 2 **Figure 1: The study area is located in the northern part of the Cuvelai-Etoshia-Basin (CEB),**  
 3 **which is subdivided by the political border between Angola and Namibia (left). Sampling was**  
 4 **conducted in Elundu located in the center of the CEB (center, right).**

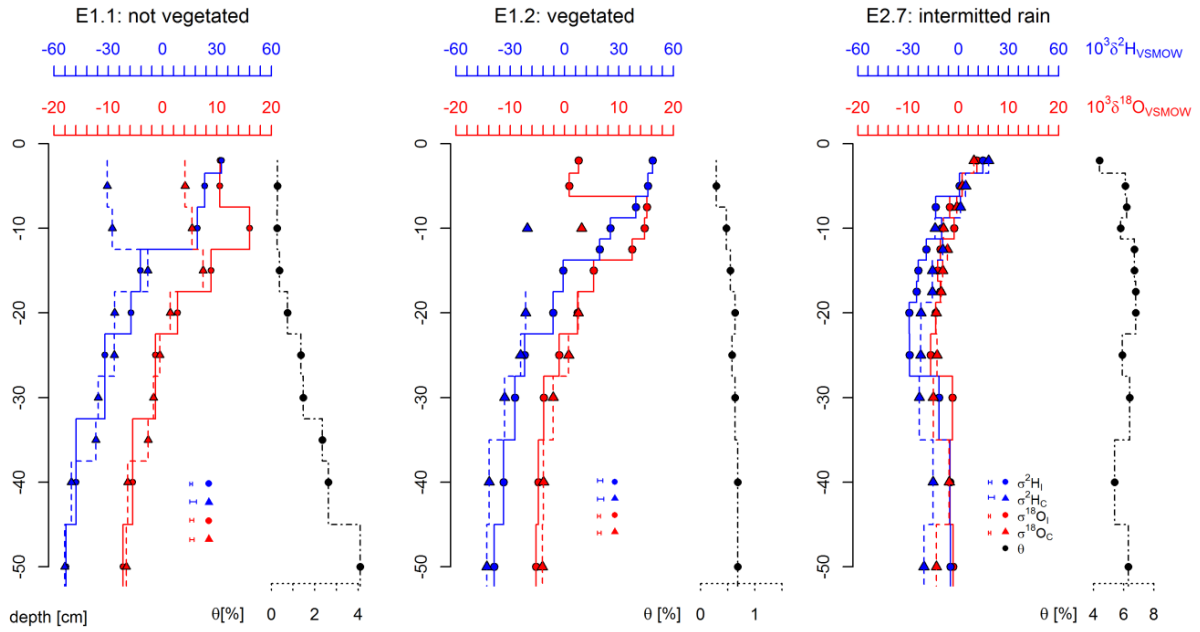
1



2

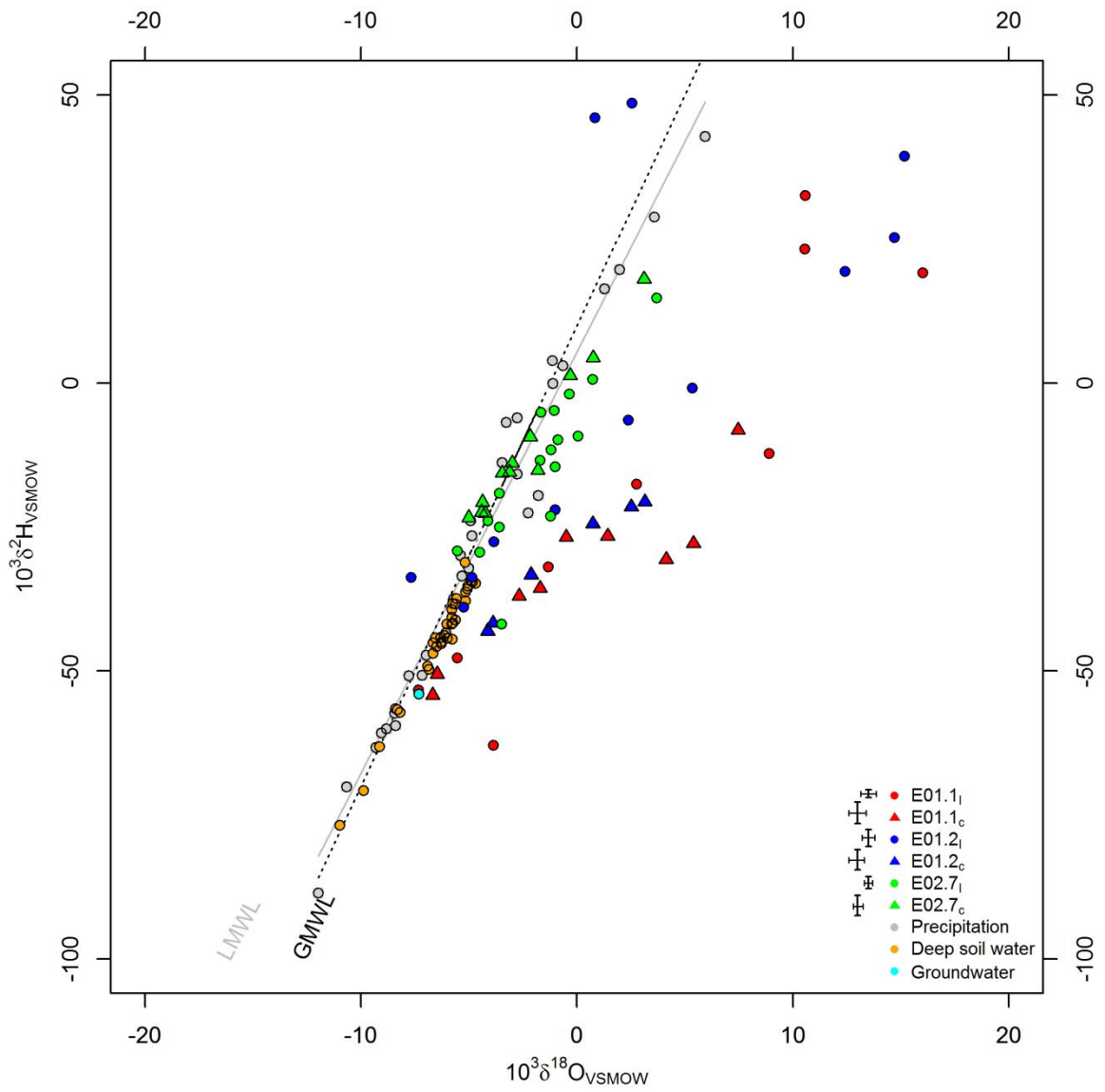
3 **Figure 2: Gas transport (right) is controlled by an automated electronic control (left). The PC**  
4 **mimics the behavior of a laboratory autosampler communicating with the analyser via an USBto**  
5 **Serial adapter. High and low signals from the data set ready pin can be used to switch valves**  
6 **using an optocoppler (ULN2303). Vapor is transported via the transport line from the soil gas**  
7 **probe to the ICOS device. The flow is measured with a massflowcontroller (MFC).**

1



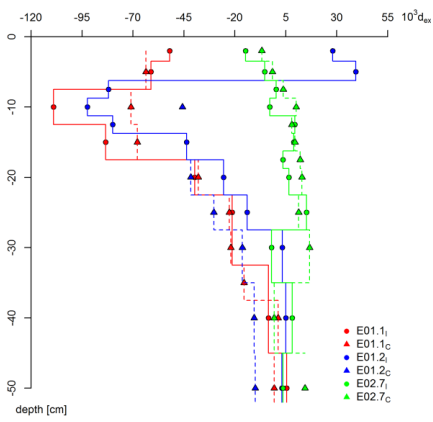
2

3 **Figure 3: Depths profiles of the field campaign in June 2014 (E1.1, E1.2) and the field campaign**  
4 **in November 2014 (E2.7) are shown. Compared are isotope depth profiles extracted with the**  
5 **cryogenic vacuum extraction (dashed, triangles) and measured in-situ (straight, dots).  $\delta^2 H$  is**  
6 **given in blue and  $\delta^{18} O$  is given in red. Soil moisture is illustrated on the right of each plot.**  
7 **Standard deviation of each plot for each method are indicated by error bars in the legend of the**  
8 **plot.**



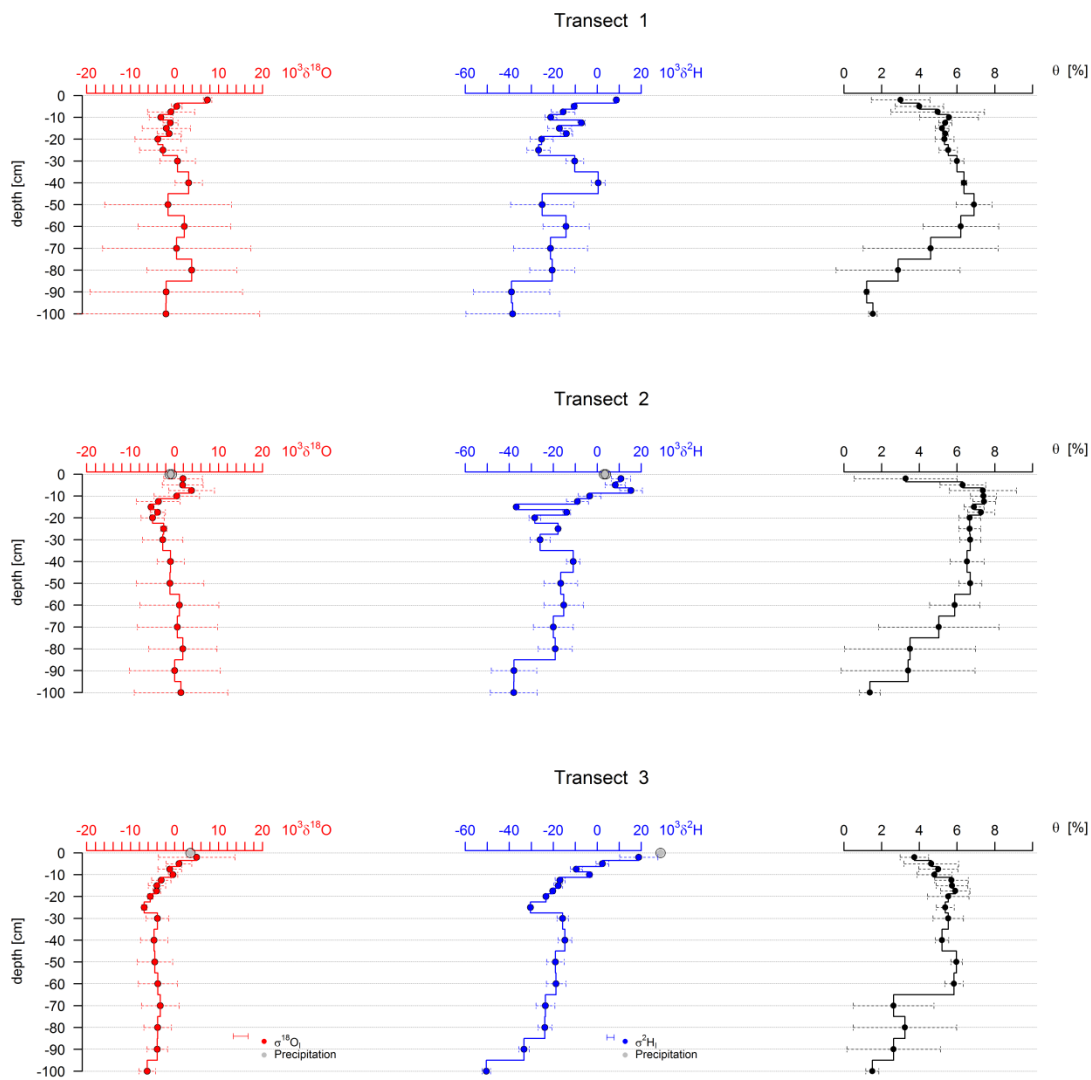
1

2 **Figure 4:  $\delta^{18}O$  vs  $\delta^2H$  plot of the profiles E01.1, E01.2, E02.7. Also shown is the LMWL for the**  
 3 **northern part of Namibia as well as groundwater and soil water down to a depth of 4 m.**



4

1 **Figure 5: Deuterium excess for the profiles E01.1, E01.2 sampled in June 2014 and E02.7**  
2 **sampled in November 2014. Compared are values from the cryogenic vacuum extraction**  
3 **(triangles) and the in-situ measurements (circles).**  
4

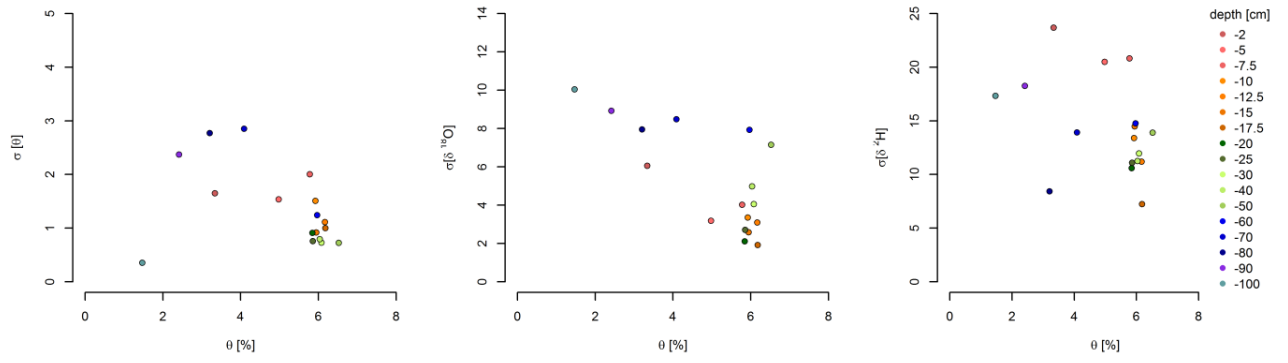


1

2 **Figure 6:  $^{18}\text{O}$  (red),  $^2\text{H}$  (blue) and soil moisture (black) depth profiles. Shown are mean values**  
 3 **for three transects consisting of three single profiles derived from in-situ measurements. Mean**  
 4 **standard deviation  $\sigma$  of all quality check standards (qc) are shown in the legend. Rainfall isotope**  
 5 **values are indicated on the x-axes in grey.**

6





1

2 **Figure 7: Mean soil moisture ( $z\Theta$ ) of each depth plotted against the standard deviation  $\sigma[\Theta]$**   
 3 **between each depth as well as standard deviation of  $\sigma[\delta^{18}\text{O}]$  and  $\sigma[\delta^2\text{H}]$ .**

4

## 1   **7   References**

- 2   Abramova, M. M.: Movement of moisture as a liquid and vapour in soils of semi-deserts  
3   (Publication 83), 781–789, 1969.
- 4   Agam, N. and Berliner, P. R.: Dew formation and water vapor adsorption in semi-arid  
5   environments - A review, *Journal of Arid Environments* (4), 572–590,  
6   doi:10.1016/j.jaridenv.2005.09.004, 2006.
- 7   Barnes, C. J. and Allison, G. B.: Tracing of Water Movement in the unsaturated zone using  
8   stable isotopes of hydrogen and oxygen, *Journal of Hydrology* (100), 143–176, 1988.
- 9   Braud, I., Bariac, T., Biron, P., and Vauclin, M.: Isotopic composition of bare soil evaporated  
10   water vapor. Part II: Modeling of RUBIC IV experimental results, *Journal of Hydrology*, 369  
11   (1-2), 17–29, doi:10.1016/j.jhydrol.2009.01.038, 2009.
- 12   Braud, I., Bariac, T., Vauclin, M., Boujamlaoui, Z., Gaudet, J. P., Biron, P., and Richard, P.:  
13   SiSPAT-Isotope, a coupled heat, water and stable isotope (HDO and H<sub>2</sub>18O) transport model  
14   for bare soil. Part II. Evaluation and sensitivity tests using two laboratory data sets, *Journal of*  
15   *Hydrology* (309), 301–320, doi:10.1016/j.jhydrol.2004.12.012, 2005.
- 16   Clark, I. D. and Fritz, P.: *Environmental Isotopes in Hydrogeology*, Lewis Publishers, 1997.
- 17   Henschel, J. R., Seely, M. K., Henschel, J. R., and Seely, M. K.: Ecophysiology of  
18   atmospheric moisture in the Namib Desert., *Atmospheric Research*, 87 (87 // 3-4), 362–368,  
19   doi:10.1016/j.atmosres.2007.11.015, 2008.
- 20   van Geldern, R. and Barth, J. A.: Optimization of instrument setup and post-run corrections  
21   for oxygen and hydrogen stable isotope measurements of water by isotope ratio infrared  
22   spectroscopy (IRIS), *Limnol. Oeangr. Methods* (10), 1024–1036,  
23   doi:10.4319/lom.2012.10.1024, 2012.